

AN INTEGRAL METHOD FOR SOLVING THE BOUNDARY-LAYER EQUATIONS FOR A
SECOND-ORDER VISCOELASTIC LIQUID

by

Clarence Wesley Kitchens, Jr.

Thesis submitted to the Graduate Faculty of the
Virginia Polytechnic Institute
in candidacy for the degree of

MASTER OF SCIENCE

in

ENGINEERING MECHANICS

APPROVED:

Chairman, D.T. Mook

R. T. Davis

C. W. Smith

August 1967

Blacksburg, Virginia

II. TABLE OF CONTENTS

	Page
I. TITLE	1
II. TABLE OF CONTENTS	2
III. LIST OF FIGURES	4
IV. LIST OF TABLES.	6
V. LIST OF SYMBOLS	7
VI. INTRODUCTION.	9
VII. LITERATURE REVIEW	11
VIII. AN INTEGRAL METHOD FOR SOLVING THE BOUNDARY-LAYER EQUATIONS FOR A SECOND-ORDER VISCOELASTIC LIQUID. .	14
1. Derivation of the Governing Differential Equations	14
2. Determination of Stagnation Values of the Dependent Variables	24
3. Solution of the Coupled Differential Equations	27
4. Application of the Governing Equations to Problems of Second-Order Flow Past a Circular Cylinder and Second-Order Flow Past a Sphere. .	35
5. Discussion of Results	38
IX. LIST OF REFERENCES	56
X. ACKNOWLEDGEMENTS	58

	Page
XI. VITA	59
APPENDIX A	60
APPENDIX B	66

III. LIST OF FIGURES

Figure	Page
1. Coordinate System	15
2. Stagnation-Point Skin Friction Variation with $\bar{\theta}$ and $\bar{\omega}$	43
3. Axisymmetric Stagnation-Point Skin Friction Variation with $\bar{\theta}$ and $\bar{\omega}$	44
4. Comparison of Exact and Approximate Wall Shear Stress for Newtonian Flow Past a Circular Cylinder.	45
5. Comparison of Wall Shear Stress for Newtonian and Second-Order Flow Past a Circular Cylinder.	46
6. Comparison of Boundary-Layer Thickness for Newtonian and Second-Order Flow Past a Circular Cylinder	47
7. Comparison of Velocity Profiles for Newtonian and Second-Order Flow Past a Circular Cylinder.	48
8. Comparison of Wall Shear Stress for Newtonian and Second-Order Flow Past a Sphere	49
9. Comparison of Wall Shear Stresses for Newtonian and Second-Order Flow Past a Sphere with $\bar{\omega} = 0.00$	50
10. Comparison of Wall Shear Stress for Newtonian and Second-Order Flow Past a Sphere with $\bar{\theta} = 0.00$	51

III. LIST OF FIGURES (CONT'D)

Figure	Page
11. Comparison of Boundary-Layer Thicknesses for Newtonian and Second-Order Flow Past a Sphere with $\bar{\omega} = 0.00$	52
12. Comparison of Boundary-Layer Thicknesses for Newtonian and Second-Order Flow Past A Sphere with $\bar{\theta} = 0.00$	53
13. Drag Ratios for Flow Past a Sphere and Flow Past a Circular Cylinder	54
14. Comparison of Separation Points for Newtonian and Second-Order Flows.	55

IV. LIST OF TABLES

Table	Page
A Numerical Results for Plane Stagnation-Point Flows	40
B Numerical Results for Axisymmetric Stagnation-Point Flows	41

V. LIST OF SYMBOLS

(a,b,c,d)	Coefficients of fourth-order polynomial
a_0	Nose radius of curvature
D	Boundary-layer thickness
$f''(0)$	Skin-friction function
j	0 for plane flow, 1 for axisymmetric flow
K	Constant
N	Normal distance measured from the body surface
P_e	Inviscid surface pressure
r_0	Body transverse radius of curvature for axisymmetric bodies
S	Curvilinear length measured along the body surface from the stagnation point
u,v	Velocity components
u_e	Inviscid velocity
u_∞	Uniform free stream velocity
δ^*	Displacement thickness
ϵ^2	1/Reynolds Number
ζ^*	$= \int_0^{\infty} \left[\frac{\partial}{\partial N} \left(\frac{u}{u_e} \right) \right]^2 dN$
η, β, γ	Material constants
$\bar{\Theta}$	First-order term in $\Theta, \frac{\Theta}{\epsilon^2}$
Θ^*	Momentum thickness

ρ	Density
τ_w	Shear stress at wall
ϕ_1, ϕ_2	Non-Newtonian viscosity coefficients
ω, θ	Second-order viscosity coefficients
$\bar{\omega}$	First-order term in ω , $\frac{\omega}{\epsilon^2}$
∇	Del operator
$()^T$	Transpose
$()^n$	Power
$\frac{D}{Dt}$	Material derivative
$\underline{\underline{I}}$	Identity tensor
$\underline{\underline{S}}$	Stress tensor

VI. INTRODUCTION

Exact solutions of the laminar boundary-layer equations for Newtonian fluids involve considerable mathematical difficulties. The problems which have been solved represent very special cases. Thus far, few exact solutions exist for problems of second-order viscoelastic flow past external surfaces and these shapes are very special cases.

For the Newtonian case, approximate methods have been devised which satisfy the differential equations of the boundary-layer only in the average and over the boundary-layer thickness. These approximate methods, satisfying the governing equations in the average, are developed from the Momentum Theorem. The Karman-Pohlhausen Method [11], for the Newtonian fluid, obtains a mean value function as an integral of the equations of motion over the boundary-layer thickness.

The purpose of this thesis is to develop an approximate method for treating two-dimensional and axisymmetric boundary layer flows of second-order fluids with pressure gradients. The integral relations thus developed can be used to find the solutions for plane and axisymmetric stagnation flows. These solutions will be tabulated and are a first step in any step-by-step integration scheme over a body contour.

The problems of second-order flow past a circular cylinder and second-order flow past a sphere will then be solved by the approximate method, as examples. Other problems can be solved using this approximate method.

VII. LITERATURE REVIEW

In the area of Non-Newtonian fluids an analog of the Navier-Stokes equations, obeyed by all fluids in motion, cannot be written down. Theoretical studies in this area are therefore limited, not so much by the mathematical complexity of the equations, as by the inability to arrive at their correct form.

Several authors have attempted to analyze the flow of Non-Newtonian fluids past external surfaces using various models to describe the relationship between stress and strain.

Using a "power-law model" to describe the stress-strain rate relationship of a Non-Newtonian fluid, where

$$\tau_w = K \left(\frac{\partial u}{\partial N} \right)^n$$

Acrivos, Shah and Petersen [1] presented an analysis for flow past a horizontal flat plate. Kapur and Srivastava [2] have obtained similar solutions of the boundary-layer equations for flow past a flat plate and flow past a wedge.

Using a model formulated by Reiner [3] to describe the stress-strain rate relationship of a Non-Newtonian fluid, where

$$\underline{\underline{S}} = -p \underline{\underline{I}} + \phi_1 \underline{\underline{A}}_{(1)} + \phi_2 \left(\underline{\underline{A}}_{(1)} \cdot \underline{\underline{A}}_{(1)} \right);$$

solutions have been presented by Nanda [4] for similar solutions of the three dimensional boundary-layer equations, by Srivastava [5] for stagnation-point flows, and by Datta [6] and by

Rajeswari [7] for rotating spheres.

Coleman and Noll [8] have derived a constitutive equation which, to the second-order, gives corrections for a general viscoelastic liquid. It is more general than those used previously to describe a viscoelastic liquid.

The constitutive equation describing the second-order fluid is given by,

$$\underline{S} = -p \underline{I} + \epsilon^2 \underline{A}_{(1)} + \omega \underline{A}_{(1)} \cdot \underline{A}_{(1)} - \theta \underline{A}_{(2)}$$

Where,

$$\epsilon^2 = \frac{\eta}{\mu_0 a_0 \rho}$$

$$\omega = \frac{\beta}{\rho a_0^2}$$

and

$$\theta = \frac{-\gamma}{\rho a_0^2}$$

Also,

$$\underline{A}_{(1)} = \nabla \underline{\hat{v}} + (\nabla \underline{\hat{v}})^T$$

and

$$\underline{A}_{(2)} = \underline{A}_{(1)} \cdot (\nabla \underline{\hat{v}})^T + [\underline{A}_{(1)} \cdot (\nabla \underline{\hat{v}})^T]^T + \frac{D}{Dt} (\underline{A}_{(1)})$$

From thermodynamic considerations [9], θ must always be zero or positive; whereas ω can be either positive, negative, or zero.

The model formulated by Reiner [3] can be obtained from this equation by letting θ equal zero. The "power-law model," however, cannot be obtained from this constitutive equation.

Merkovitz and Coleman [9] have used the constitutive equation of Coleman and Noll to solve several simple flow problems.

Davis [10], using this constitutive equation for a second-order fluid, has derived a set of boundary-layer equations for uniform flow past plane and axisymmetric bodies in physical variables. He has presented them in integral form and in von Mises variables. Davis also presents solutions for stagnation-point flows (plane and axisymmetric) and for flow past a flat plate.

VIII. AN INTEGRAL METHOD FOR SOLVING THE BOUNDARY LAYER EQUATIONS FOR A SECOND-ORDER VISCOELASTIC LIQUID

1. Derivation of the Governing Differential Equations

In this section, the equations governing the second-order fluid will be used to develop an approximate method for solving the boundary-layer equations for both plane and axisymmetric flows.

Davis has shown [10] that the momentum integral equation for a second-order fluid can be written:

$$\begin{aligned} \frac{\partial}{\partial t} (\mu_e \delta^*) + \mu_e^2 \frac{\partial}{\partial s} (\theta^* + 2\bar{\theta} \zeta^*) \\ + \mu_e \frac{\partial \mu_e}{\partial s} [\delta^* + 2(\theta^* + 2\bar{\theta} \zeta^*)] \\ + \frac{d}{ds} (\ln r_0^j) \mu_e^2 (\theta^* + \bar{\omega} \zeta^*) = \tau_w - \bar{\theta} \frac{\partial \tau_w}{\partial t}. \end{aligned} \quad (1.01)$$

The boundary-layer thicknesses are defined as follows:

$$\zeta^* = \int_0^{\infty} \left[\frac{\partial}{\partial N} \left(\frac{\mu}{\mu_e} \right) \right]^2 dN. \quad (1.02)$$

ζ^* is a new thickness not appearing in the equations for Newtonian flow.

$$\delta^* = \int_0^{\infty} \left(1 - \frac{\mu}{\mu_e} \right) dN, \quad (1.03)$$

the usual definition for the displacement thickness δ^* , and

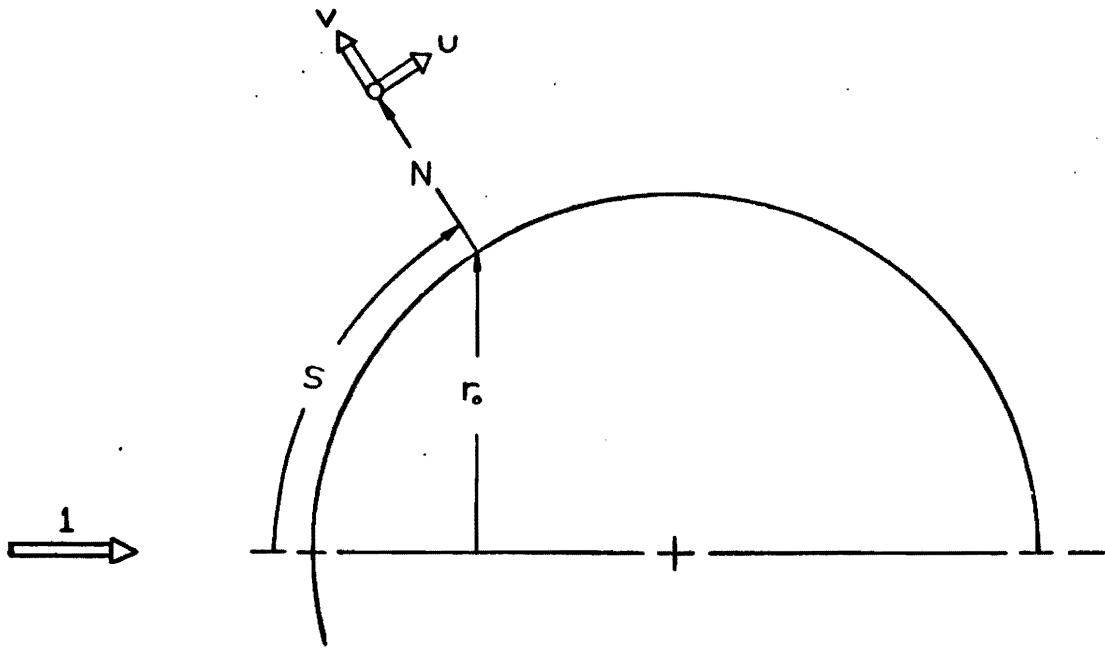


Figure 1 - Coordinate System

$$\Theta^* = \int_0^{\infty} \frac{\mu}{\mu_e} \left(1 - \frac{\mu}{\mu_e} \right) dN, \quad (1.04)$$

the usual definition for the momentum thickness Θ^* .

Rewriting (1.01), and considering steady flow only, we obtain

$$\begin{aligned} \mu_e^2 \left(\frac{d\Theta^*}{ds} + 2\bar{\Theta} \frac{d\psi^*}{ds} \right) + \mu_e \frac{d\mu_e}{ds} (\delta^* + 2\Theta^* + 4\bar{\Theta}\psi^*) \\ + \frac{d}{ds} (\bar{\omega} r_o^j) \mu_e^2 (\Theta^* + \bar{\omega}\psi^*) = \tau_w. \end{aligned} \quad (1.05)$$

Equation (1.05) shows that the effect of the $\bar{\omega}$ term appears only for axisymmetric flow.

Pohlhausen has shown [11] that assuming a fourth-order polynomial to describe the boundary-layer velocity profile leads to results in good agreement with the exact solution for the Newtonian fluid. To extend this technique for a second-order fluid, a fourth-order polynomial of the following form will be assumed.

$$\frac{\mu}{\mu_e} = a \left(\frac{N}{D} \right) + b \left(\frac{N}{D} \right)^2 + c \left(\frac{N}{D} \right)^3 + d \left(\frac{N}{D} \right)^4. \quad (1.06)$$

For $\frac{N}{D} \cong 1$, we assume $\frac{\mu}{\mu_e} = 1$. When $N=D(s)$, it is assumed that the boundary-layer has joined the potential flow.

To determine the four unknown functions of $s(a, b, c, d)$, the following boundary conditions will be prescribed.

At $N=0$,

$$\mu = v = 0. \quad (1.07)$$

At $N=D$,

$$\mu = \mu_e, \quad (1.08)$$

$$\frac{\partial \mu}{\partial N} = 0, \quad (1.09)$$

and

$$\frac{\partial^2 \mu}{\partial N^2} = 0. \quad (1.10)$$

The continuity equation can be written

$$\frac{\partial}{\partial S} (r_o^j \mu) + \frac{\partial}{\partial N} (r_o^j v) = 0. \quad (1.11)$$

It was also shown [10] that the s-Momentum equation for steady flow is

$$\begin{aligned} \mu \frac{\partial \mu}{\partial S} + v \frac{\partial \mu}{\partial N} = & - \frac{dP_e}{dS} + \frac{\partial^2 \mu}{\partial N^2} - (\bar{\omega} - 2\bar{\theta}) \frac{\partial}{\partial S} \left(\frac{\partial \mu}{\partial N} \right)^2 \\ & + \frac{\bar{\omega}}{r_o^j} \frac{\partial}{\partial S} \left[r_o^j \left(\frac{\partial \mu}{\partial N} \right)^2 \right] + 2\bar{\omega} \frac{\partial}{\partial N} \left[\frac{\partial \mu}{\partial N} \left(\frac{\partial \mu}{\partial S} + \frac{\partial v}{\partial N} \right) \right] \\ & - \bar{\theta} \frac{\partial}{\partial N} \left[\mu \frac{\partial^2 \mu}{\partial S \partial N} + v \frac{\partial^2 \mu}{\partial N^2} + \frac{\partial \mu}{\partial N} \left(3 \frac{\partial \mu}{\partial S} + \frac{\partial v}{\partial N} \right) \right]. \end{aligned} \quad (1.12)$$

The continuity equation (1.11) can be rewritten

$$\frac{\partial \mu}{\partial S} + \frac{\partial v}{\partial N} = - \frac{r_o^{j'}}{r_o^j} (\mu). \quad (1.13)$$

Applying condition (1.07) to (1.13), at $N=0$ the continuity equation reduces to

$$\frac{\partial \mu}{\partial S} = - \frac{\partial v}{\partial N}. \quad (1.14)$$

The s-Momentum equation can similarly be rewritten at $N=0$ by applying condition (1.07) to (1.12).

$$\begin{aligned} \frac{dP_e}{dS} = & \frac{\partial^2 \mu}{\partial N^2} - (\bar{\omega} - 2\bar{\theta}) \frac{\partial}{\partial S} \left(\frac{\partial \mu}{\partial N} \right)^2 + \frac{\bar{\omega}}{r_o^j} \frac{\partial}{\partial S} \left[r_o^j \left(\frac{\partial \mu}{\partial N} \right)^2 \right] \\ & + 2\bar{\omega} \frac{\partial}{\partial N} \left[\frac{\partial \mu}{\partial N} \left(\frac{\partial \mu}{\partial S} + \frac{\partial v}{\partial N} \right) \right] - \bar{\theta} \left[\frac{\partial \mu}{\partial N} \frac{\partial^2 \mu}{\partial S \partial N} + \frac{\partial v}{\partial N} \frac{\partial^2 \mu}{\partial N^2} \right] \\ & + \frac{\partial^2 \mu}{\partial N^2} \left(3 \frac{\partial \mu}{\partial S} + \frac{\partial v}{\partial N} \right) + \frac{\partial \mu}{\partial N} \left(3 \frac{\partial^2 \mu}{\partial S \partial N} + \frac{\partial^2 v}{\partial N^2} \right). \end{aligned} \quad (1.15)$$

Carrying out the differentiation of (1.15),

$$\begin{aligned} \frac{dP_e}{ds} &= \frac{\partial^2 \mu}{\partial N^2} + \bar{\omega} \left(\frac{\partial \mu}{\partial N} \right)^2 \frac{r_o j'}{r_o j} + 2 \bar{\omega} \frac{\partial}{\partial N} \left[\frac{\partial \mu}{\partial N} \left(\frac{\partial \mu}{\partial S} + \frac{\partial V}{\partial N} \right) \right] \\ &- \bar{\Theta} \left[2 \frac{\partial V}{\partial N} \frac{\partial^2 \mu}{\partial N^2} + 3 \frac{\partial \mu}{\partial S} \frac{\partial^2 \mu}{\partial N^2} + \frac{\partial \mu}{\partial N} \frac{\partial^2 V}{\partial N^2} \right]. \end{aligned} \quad (1.16)$$

Applying the result from the continuity equation (1.14),

$$\frac{dP_e}{ds} = \frac{\partial^2 \mu}{\partial N^2} - \bar{\omega} \left(\frac{\partial \mu}{\partial N} \right)^2 \frac{r_o j'}{r_o j} - \bar{\Theta} \left[- \frac{\partial V}{\partial N} \frac{\partial^2 \mu}{\partial N^2} + \frac{\partial \mu}{\partial N} \frac{\partial^2 V}{\partial N^2} \right]. \quad (1.17)$$

It can be shown from Bernoulli's equation that

$$\frac{dP_e}{ds} = -\mu_e \frac{d\mu_e}{ds}. \quad (1.18)$$

Rewriting (1.17), using (1.18),

$$-\mu_e \frac{d\mu_e}{ds} = \frac{\partial^2 \mu}{\partial N^2} - \bar{\omega} \left(\frac{\partial \mu}{\partial N} \right)^2 \frac{r_o j'}{r_o j} - \bar{\Theta} \left[- \frac{\partial V}{\partial N} \frac{\partial^2 \mu}{\partial N^2} + \frac{\partial \mu}{\partial N} \frac{\partial^2 V}{\partial N^2} \right]. \quad (1.19)$$

At the body surface $N=0$, we know $\frac{\partial \mu}{\partial S} = 0$. Therefore, from (1.14) we can conclude that at the body surface

$$\frac{\partial V}{\partial N} = 0. \quad (1.20)$$

Equation (1.19) can thus be simplified using (1.20),

$$\frac{\partial^2 \mu}{\partial N^2} = -\mu_e \frac{d\mu_e}{ds} + \bar{\omega} \left(\frac{\partial \mu}{\partial N} \right)^2 \frac{r_o j'}{r_o j} + \bar{\Theta} \left(\frac{\partial \mu}{\partial N} \frac{\partial^2 V}{\partial N^2} \right). \quad (1.21)$$

We will be able to further simplify (1.21) if we use the result obtained by differentiating the continuity equation (1.13) with respect to N ,

$$\frac{\partial^2 V}{\partial N^2} = \frac{r_o j'}{r_o j} \left(\frac{\partial \mu}{\partial N} \right) - \frac{\partial^2 \mu}{\partial S \partial N}. \quad (1.22)$$

Substituting (1.22) into (1.21),

$$\frac{\partial^2 \mu}{\partial N^2} = -\mu_e \frac{d\mu_e}{ds} - (\bar{\theta} - \bar{\omega}) \left(\frac{\partial \mu}{\partial N} \right)^2 \frac{r_0^j}{r_0} - \bar{\theta} \left(\frac{\partial \mu}{\partial N} \right) \left(\frac{\partial^2 \mu}{\partial s \partial N} \right). \quad (1.23)$$

Equation (1.06) can be differentiated with respect to N to obtain,

$$\frac{1}{\mu_e} \left(\frac{\partial \mu}{\partial N} \right) = a \left(\frac{1}{D} \right) + 2b \left(\frac{N}{D^2} \right) + 3c \left(\frac{N^2}{D^3} \right) + 4d \left(\frac{N^3}{D^4} \right). \quad (1.24)$$

Differentiating again,

$$\frac{1}{\mu_e} \left(\frac{\partial^2 \mu}{\partial N^2} \right) = 2b \left(\frac{1}{D^2} \right) + 6c \left(\frac{N}{D^3} \right) + 12d \left(\frac{N^2}{D^4} \right). \quad (1.25)$$

By applying the boundary conditions (1.08), (1.09), (1.11) to (1.06), (1.24) and (1.25) respectively, we obtain the three algebraic equations

$$1 = a + b + c + d, \quad (1.26)$$

$$0 = a + 2b + 3c + 4d, \quad (1.27)$$

and

$$0 = 2b + 6c + 12d. \quad (1.28)$$

Writing (1.24) at $N = 0$,

$$\frac{\partial \mu}{\partial N} = \frac{\mu_e a}{D}. \quad (1.29)$$

Differentiating with respect to s , since a , D , and μ_e are functions of s only,

$$\frac{\partial^2 \mu}{\partial s \partial N} = \left(\frac{a}{D} \right) \frac{d\mu_e}{ds} + \left(\frac{\mu_e}{D} \right) \frac{da}{ds} - \left(\frac{\mu_e a}{D^2} \right) \frac{dD}{ds}. \quad (1.30)$$

Writing (1.25) at $N=0$,

$$\frac{\partial^2 \mu}{\partial N^2} = \frac{2b\mu_e}{D^2} . \quad (1.31)$$

Substituting (1.29), (1.30), (1.31) into the S -momentum equation (1.23),

$$\begin{aligned} 0 = & 2b + D^2 \frac{d\mu_e}{ds} + (\bar{\theta} - \bar{\omega}) a^2 \mu_e \frac{r_{0j}^{j'}}{r_{0j}} + \bar{\theta} \left[a^2 \frac{d\mu_e}{ds} \right. \\ & \left. + a \mu_e \frac{da}{ds} - \left(\frac{a^2 \mu_e}{D} \right) \frac{dD}{ds} \right] . \end{aligned} \quad (1.32)$$

The three algebraic equations (1.26), (1.27) and (1.28) can be solved simultaneously to express three of the unknowns (b,c,d) as functions of the fourth (a) , yielding:

$$b = 6 - 3a , \quad (1.33)$$

$$c = -8 + 3a , \quad (1.34)$$

and

$$d = 3 - a . \quad (1.35)$$

Equation (1.33) can now be substituted into (1.32), expressing the S -momentum equation as an ordinary differential equation in terms of two unknown quantities a and D , both functions of S only. Equation (1.32) becomes

$$\begin{aligned} \left[\bar{\theta} \left(\frac{\mu_e a^2}{D} \right) \right] \frac{dD}{ds} - \left[\bar{\theta} a \mu_e \right] \frac{da}{ds} = & 12 - 6a \\ + (\bar{\theta} - \bar{\omega}) a^2 \mu_e \frac{r_{0j}^{j'}}{r_{0j}} + (\bar{\theta} a^2 + D^2) \frac{d\mu_e}{ds} . \end{aligned} \quad (1.36)$$

We have thus obtained from the S -momentum equation, one ordinary differential equation which is a function of two variables, α and D . Using the momentum integral equation (1.05), we will be able to obtain another ordinary differential equation which is a function of the same two variables. These coupled equations may then be solved simultaneously, yielding approximate solutions to the boundary layer equations.

To express the momentum integral equation as a function of α and D , we must first express the boundary-layer thicknesses as functions of α and D . Substituting the fourth-order polynomial describing the velocity profile (1.06) into the expression for the displacement thickness δ^* (1.03) and carrying out the integration, we obtain

$$\delta^* = D \left[1 - \alpha \left(\frac{1}{2} \right) - b \left(\frac{1}{3} \right) - c \left(\frac{1}{4} \right) - d \left(\frac{1}{5} \right) \right]. \quad (1.37)$$

Now substituting (1.33), (1.34), (1.35), the displacement thickness becomes a function of two variables, α and D ,

$$\delta^* = \frac{D}{20} [8 - \alpha]. \quad (1.38)$$

By a similar procedure, we can obtain

$$\theta^* = D \left[-\frac{\alpha^2}{252} + \frac{\alpha}{105} + \frac{4}{35} \right], \quad (1.39)$$

and

$$\zeta^* = \frac{1}{35D} [3\alpha^2 - 4\alpha + 48]. \quad (1.40)$$

The shear stress at the wall τ_w can be obtained from (1.29) and equals

$$\tau_w = \frac{\mu_e a}{D} . \quad (1.41)$$

Now, substituting (1.38), (1.39), (1.40) and (1.41) into the momentum integral equation (1.05), we obtain

$$\begin{aligned} \mu_e^2 \left\{ \frac{d}{ds} \left[\left(-\frac{a^2}{252} + \frac{a}{105} + \frac{4}{35} \right) D \right] + 2\bar{\theta} \frac{d}{ds} \left[(3a^2 - 4a \right. \right. \\ \left. \left. + 48) \frac{1}{35D} \right] \right\} + \mu_e \frac{d\mu_e}{ds} \left[\frac{D}{20} (8-a) + 2 \left(-\frac{a^2}{252} + \frac{a}{105} \right. \right. \\ \left. \left. + \frac{4}{35} \right) D + 4\bar{\theta} (3a^2 - 4a + 48) \frac{1}{35D} \right] + \frac{d}{ds} (\ln r_0^j) \mu_e^2 \left[\left(-\frac{a^2}{252} \right. \right. \\ \left. \left. + \frac{a}{105} + \frac{4}{35} \right) D + \bar{\omega} (3a^2 - 4a + 48) \frac{1}{35D} \right] = \frac{\mu_e a}{D} . \end{aligned} \quad (1.42)$$

Carrying out the differentiation in (1.42) and simplifying,

$$\begin{aligned} \left[\left(-\frac{a^2}{252} + \frac{a}{105} + \frac{4}{35} \right) - \frac{2\bar{\theta}}{35D^2} (3a^2 - 4a + 48) \right] \frac{dD}{ds} \\ + \left[D \left(-\frac{a}{126} + \frac{1}{105} \right) + \frac{2\bar{\theta}}{35D} (6a - 4) \right] \frac{da}{ds} = \\ - \left[\frac{d\mu_e}{ds} / \mu_e \right] \left[\frac{D}{20} (8-a) + 2D \left(-\frac{a^2}{252} + \frac{a}{105} + \frac{4}{35} \right) \right. \\ \left. + \frac{4\bar{\theta}}{35D} (3a^2 - 4a + 48) \right] - \frac{d}{ds} (\ln r_0^j) \left[D \left(-\frac{a^2}{252} \right. \right. \\ \left. \left. + \frac{a}{105} + \frac{4}{35} \right) + \frac{\bar{\omega}}{35D} (3a^2 - 4a + 48) \right] + \frac{a}{\mu_e D} . \end{aligned} \quad (1.43)$$

Equation (1.43) now gives us a second ordinary differential equation which is coupled to (1.36). Since attempting to uncouple these equations appears to be a hopeless task, the use of a numerical technique for their simultaneous solution appears to be the most logical method. It will first be necessary to determine the stagnation values for a , D and their derivatives since these values are used as initial values for a step-by-step integration along the body contour.

2. Determination of Stagnation Values of the Dependent Variables

In order to apply equations (1.36) and (1.43) to solve for the unknowns describing the boundary-layer profile for flow over symmetric bodies, the values of α and D must be determined at the stagnation point on the body. The stagnation values can then be used as first points for a step-by-step numerical integration along the body contour.

Since flow over symmetric bodies is of principal interest, the variables in the momentum integral equation (1.05) can be expanded in the following form:

$$\theta^* = \theta_1^* + \theta_2^* S^2 + \dots , \quad (2.01)$$

$$\delta^* = \delta_1^* + \delta_2^* S^2 + \dots , \quad (2.02)$$

$$\zeta^* = \zeta_1^* + \zeta_2^* S^2 + \dots , \quad (2.03)$$

$$\tau_w = \tau_{1w} S + \tau_{2w} S^2 + \dots , \quad (2.04)$$

$$\mu = \mu_1 S + \dots , \quad (2.05)$$

$$\mu_e = \mu_1 S + \dots , \quad (2.06)$$

and

$$r_o^j = S^j + \dots . \quad (2.07)$$

Now substituting (2.01) thru (2.04), (2.06) and (2.07) into the momentum integral equation (1.05), carrying out the differentiation and keeping only the lowest-order terms in S ,

$$\mu_1^2 [\delta_1^* + 2\theta_1^* + 4\bar{\omega} \zeta_1^*] + j \mu_1^2 [\theta_1^* + \bar{\omega} \zeta_1^*] = \tau_{1w} . \quad (2.08)$$

Rewriting (2.08) in terms of a and D , using (1.38) thru (1.41),

$$D^2 \mu_1 \left[\frac{1}{20}(8-a) + (j+2) \left(-\frac{a^2}{252} + \frac{a}{105} + \frac{4}{35} \right) \right] + \mu_1 \left[\frac{(4\bar{\theta} + j\bar{\omega})}{35} (3a^2 - 4a + 48) \right] - a = 0. \quad (2.09)$$

This thus gives us one algebraic equation obtained from the momentum integral equation. A second algebraic equation comes from the S -momentum equation written at $N=0$ (1.23).

$$\frac{\partial^2 \mu}{\partial N^2} = -\mu_e \frac{d\mu_e}{ds} - (\bar{\theta} - \bar{\omega}) \left(\frac{\partial \mu}{\partial N} \right)^2 \frac{r_0^{j'}}{r_0^j} - \bar{\theta} \left(\frac{\partial \mu}{\partial N} \right) \left(\frac{\partial^2 \mu}{\partial S \partial N} \right). \quad (2.10)$$

Now using (2.05), (2.06) and (2.07), we can rewrite (2.10) as

$$\frac{\partial^2 \mu_1}{\partial N^2} = -\mu_1^2 - [j(\bar{\theta} - \bar{\omega}) + \bar{\theta}] \left(\frac{\partial \mu_1}{\partial N} \right)^2. \quad (2.11)$$

From (1.29), (1.31) and (1.33), equation (2.11) becomes

$$D^2 = -\frac{(12-6a)}{\mu_1} - a^2 [-j\bar{\omega} + (j+1)\bar{\theta}]. \quad (2.12)$$

Now substituting the second equation (2.12) into (2.09) we have an algebraic equation in terms of one unknown, a .

$$\left\{ 6a - 12 - \mu_1 a^2 [-j\bar{\omega} + (j+1)\bar{\theta}] \right\} \left\{ \frac{8-a}{20} + (j+2) \left(-\frac{a^2}{252} + \frac{a}{105} + \frac{4}{35} \right) \right\} + \mu_1 \frac{(4\bar{\theta} + j\bar{\omega})}{35} (3a^2 - 4a + 48) - a = 0. \quad (2.13)$$

This algebraic equation was solved numerically for both plane and axisymmetric stagnation flows yielding values of Ω , for various $\bar{\Theta}$ and $\bar{\omega}$. Values of D were obtained from (2.12). A non-dimensional skin friction function, $f''(0)$, defined [10] by

$$f''(0) = \frac{a(0)}{D(0)\sqrt{\mu_1}} \quad (2.14)$$

was also obtained. Tables A and B show these results for stagnation-point flows. Where possible, the exact solution for the skin friction function obtained by Davis [10] is shown for comparison. The computer program used to obtain the numerical results presented in Tables A and B is included as Appendix A.

3. Solution of the Coupled Differential Equations

Equations (1.36) and (1.43) can be solved simultaneously to obtain equations of the following form:

$$\frac{dD}{ds} = f(\alpha, D) \quad (3.01)$$

and

$$\frac{d\alpha}{ds} = g(\alpha, D) \quad (3.02)$$

With stagnation values of α and D known, (3.01) and (3.02) should easily yield values of α and D along the body contour. The use of (3.01) and (3.02) did not yield suitable results. Looking at (1.36), we see that the left hand side of this equation vanishes for small values of $\bar{\Theta}$, cancelling the effects of the derivatives of α and D in the equation (1.36). Since $\bar{\Theta}$ is assumed to be small [10] in the derivation of the boundary layer equations, a first approximation to (1.36), that will include the derivatives of α and D as a predominant effect, should be used in place of (1.36).

Rewriting (1.36), taking $\bar{\Theta}$ equal zero,

$$12 - 6\alpha - \bar{\omega} \alpha^2 \mu_e \left(\frac{r_o^{j'}}{r_o^j} \right) + D^2 \frac{d\mu_e}{ds} = 0 \quad (3.03)$$

Differentiating (3.03) with respect to S , we obtain

$$\frac{dD}{ds} = - \left[\left(\frac{1}{D \frac{d\mu_e}{ds}} \right) \left(3 + \bar{\omega} \alpha \mu_e \frac{r_o^{j'}}{r_o^j} \right) \right] \frac{d\alpha}{ds} =$$

$$\frac{\bar{\omega} a^2}{2D} \left[\frac{r_0 j'}{r_0} - \frac{\mu_e}{\frac{d\mu_e}{ds}} \left(\frac{r_0 j'}{r_0} \right)^2 \right] - \frac{D}{2} \left(\frac{d^2 \mu_e}{ds^2} \right) . \quad (3.04)$$

Rewriting (1.43), taking $\bar{\theta}$ equal zero,

$$\begin{aligned} & \left[-\frac{a^2}{252} + \frac{a}{105} + \frac{4}{35} \right] \frac{dD}{ds} + \left[D \left(-\frac{a}{126} + \frac{1}{105} \right) \right] \frac{da}{ds} = \\ & - \left[\frac{d\mu_e}{ds} \right] \left[\frac{D}{20} (8-a) + 2D \left(-\frac{a^2}{252} + \frac{a}{105} + \frac{4}{35} \right) \right] \\ & - \left[\frac{r_0 j'}{r_0} \right] \left[D \left(-\frac{a^2}{252} + \frac{a}{105} + \frac{4}{35} \right) + \frac{\bar{\omega}}{35D} (3a^2 - 4a + 48) \right] \\ & + \frac{a}{\mu_e D} . \end{aligned} \quad (3.05)$$

Equations (3.04) and (3.05) are now of the form

$$\left[F(a, D) \right] \frac{dD}{ds} + \left[G(a, D) \right] \frac{da}{ds} = T(a, D) \quad (3.06)$$

and

$$\left[H(a, D) \right] \frac{dD}{ds} + \left[I(a, D) \right] \frac{da}{ds} = V(a, D) . \quad (3.07)$$

Solving simultaneously for the derivatives, we get

$$\frac{dD}{ds} = \frac{IT - GV}{IF - GH} \quad (3.08)$$

and

$$\frac{da}{ds} = \frac{FV - HT}{IF - GH} . \quad (3.09)$$

These derivatives thus represent a first approximation to the derivatives for small values of $\bar{\theta}$. Substituting these derivatives (3.08) and (3.09) into (1.36), we get an algebraic equation,

$$\begin{aligned}
 & \left\{ \left[\bar{\theta} \left(\frac{\mu_e a^2}{D} \right) \right] \right\} \left\{ \left[D \left(-\frac{a}{126} + \frac{1}{105} \right) \right] \left[\frac{\bar{w} a^2}{2D} \left(\frac{r_{0j}'}{r_{0j}} \right) \left(1 - \frac{d\mu_e}{ds} \frac{r_{0j}'}{r_{0j}} \right) \right. \right. \\
 & - \frac{D}{2} \left(\frac{d^2 \mu_e}{ds^2} \right) \left. \right] + \left[\left(\frac{1}{D} \frac{d\mu_e}{ds} \right) \left(3 + \bar{w} a \mu_e \frac{r_{0j}'}{r_{0j}} \right) \right] \left[\frac{a}{\mu_e D} \right. \\
 & - \left. \frac{r_{0j}'}{r_{0j}} D \left(-\frac{a^2}{252} + \frac{a}{105} + \frac{4}{35} \right) - \frac{r_{0j}'}{r_{0j}} \frac{\bar{w}}{35D} (3a^2 - 4a + 48) \right] \left. \right\} \\
 & + \left\{ \left[-\bar{\theta} a \mu_e \right] \right\} \left\{ \left[\frac{a}{\mu_e D} - \frac{r_{0j}'}{r_{0j}} D \left(-\frac{a^2}{252} + \frac{a}{105} + \frac{4}{35} \right) \right. \right. \\
 & - \left. \frac{r_{0j}'}{r_{0j}} \frac{\bar{w}}{35D} (3a^2 - 4a + 48) \right] - \left[-\frac{a^2}{252} + \frac{a}{105} + \frac{4}{35} \right] \left[\frac{\bar{w} a^2}{2D} \frac{r_{0j}'}{r_{0j}} \right. \\
 & - \left. \frac{\bar{w} a^2}{2D} \left(\frac{\mu_e}{ds} \right) \left(\frac{r_{0j}'}{r_{0j}} \right)^2 - \frac{D}{2} \left(\frac{d^2 \mu_e}{ds^2} \right) \right] \left. \right\} \\
 & + \left\{ 12 - 6a + (\bar{\theta} - \bar{w}) a^2 \mu_e \frac{r_{0j}'}{r_{0j}} + (\bar{\theta} a^2 + D^2) \frac{d\mu_e}{ds} \right\} \left\{ \frac{-1}{D} \frac{d\mu_e}{ds} \left(3 \right. \right. \\
 & \left. \left. + \bar{w} a \mu_e \frac{r_{0j}'}{r_{0j}} \right) \left[-\frac{a^2}{252} + \frac{a}{105} + \frac{4}{35} \right] - \left[D \left(-\frac{a}{126} + \frac{1}{105} \right) \right] \right\} = 0 . \\
 & \hspace{25em} (3.10)
 \end{aligned}$$

Differentiating this algebraic equation (3.10) with respect to S , we obtain the differential equation representing a first approximation to equation (1.36). This equation will be presented in parts, as

$$(R1) \frac{da}{ds} + (R2) \frac{dD}{ds} = (R3) . \hspace{15em} (3.11)$$

Where,

$$R1 = (A1)(x1) + (A2)(x2) + (A3)(x3) + (A4)(x4) + (A5)(x5) \\ + (A6)(x6) + (A7)(x7) + (A8)(x8) , \quad (3.12)$$

$$R2 = (A1)(w1) + (A3)(w2) + (A4)(w3) + (A5)(w4) + (A6)(w5) \\ + (A7)(w6) , \quad (3.13)$$

and

$$R3 = (A1)(y1) + (A2)(y2) + (A3)(y3) + (A4)(y4) + (A5)(y5) \\ + (A7)(y6) . \quad (3.14)$$

Also,

$$X1 = -6 + (\bar{\theta} - \bar{w}) 2a \mu_e \frac{r_o^{j'}}{r_o^j} + 2a \bar{\theta} \frac{d\mu_e}{ds} , \quad (3.15)$$

$$X2 = -\bar{\theta} \mu_e , \quad (3.16)$$

$$X3 = \frac{2\bar{\theta} a \mu_e}{D} , \quad (3.17)$$

$$X4 = \frac{D}{20} \frac{d\mu_e}{ds} - \frac{2D}{\mu_e} \frac{d\mu_e}{ds} \left(-\frac{a}{126} + \frac{1}{105} \right) - \frac{r_o^{j'}}{r_o^j} D \left(-\frac{a}{126} + \frac{1}{105} \right) \\ + \frac{1}{\mu_e D} - \frac{\bar{w}}{35D} \frac{r_o^{j'}}{r_o^j} (6a-4) , \quad (3.18)$$

$$X5 = \frac{\bar{w} a}{D} \frac{r_o^{j'}}{r_o^j} \left(1 - \frac{\mu_e}{\frac{d\mu_e}{ds}} \frac{r_o^{j'}}{r_o^j} \right) , \quad (3.19)$$

$$X6 = -\frac{D}{126} , \quad (3.20)$$

$$X7 = - \frac{\bar{w}}{D} \frac{r_{oj}'}{r_{oj}} \frac{\mu_e}{\frac{d\mu_e}{ds}}, \quad (3.21)$$

and

$$X8 = - \frac{a}{126} + \frac{1}{105}. \quad (3.22)$$

Also,

$$W1 = 2D \frac{d\mu_e}{ds}, \quad (3.23)$$

$$W2 = - \frac{\bar{\theta} a^2 \mu_e}{D^2}, \quad (3.24)$$

$$W3 = \frac{a-8}{20} \frac{\frac{d\mu_e}{ds}}{\mu_e} - \left(\frac{r_{oj}'}{r_{oj}} + \frac{2 \frac{d\mu_e}{ds}}{\mu_e} \right) \left(- \frac{a^2}{252} + \frac{a}{105} + \frac{4}{35} - \frac{a}{\mu_e D^2} + \frac{\bar{w}}{35 D^2} \frac{r_{oj}'}{r_{oj}} (3a^2 - 4a + 48) \right), \quad (3.25)$$

$$W4 = \left(\frac{w a^2 r_{oj}'}{2 D^2 r_{oj}} \right) \left(\frac{\mu_e}{\frac{d\mu_e}{ds}} \frac{r_{oj}'}{r_{oj}} - 1 \right) + \frac{\mu_e}{2 \frac{d\mu_e}{ds}}, \quad (3.26)$$

$$W5 = - \frac{a}{126} + \frac{1}{105}, \quad (3.27)$$

and

$$W6 = \frac{3}{D^2 \frac{d\mu_e}{ds}} + \frac{\bar{w} a}{D^2} \frac{r_{oj}'}{r_{oj}} \frac{\mu_e}{\frac{d\mu_e}{ds}}. \quad (3.28)$$

Also,

$$Y1 = (\bar{\theta} a^2 + D^2) \mu_e - (\bar{\theta} - \bar{w}) a^2 \frac{r_{oj}'}{r_{oj}} \left(\frac{d\mu_e}{ds} - \mu_e \frac{r_{oj}'}{r_{oj}} \right), \quad (3.29)$$

$$Y2 = + \bar{\theta} a \frac{d\mu_e}{ds}, \quad (3.30)$$

$$Y_3 = - \frac{\bar{\theta} a^2 \frac{d\mu_e}{ds}}{D}, \quad (3.31)$$

$$Y_4 = \frac{D(a-8)}{20} \left[\left(\frac{\frac{d\mu_e}{ds}}{\mu_e} \right)^2 + 1 \right] - D \left(-\frac{a^2}{252} + \frac{a}{105} + \frac{4}{35} \right) \left[\left(\frac{r_{0j}'}{r_{0j}} \right)^2 + 2 \left(\frac{\frac{d\mu_e}{ds}}{\mu_e} \right)^2 + 2 \right] + \frac{a \frac{d\mu_e}{ds}}{\mu_e^2 D} - \frac{\bar{w}}{35D} \left(\frac{r_{0j}'}{r_{0j}} \right)^2 (3a^2 - 4a + 48), \quad (3.32)$$

$$Y_5 = - \frac{D}{2} \left[1 + \left(\frac{\mu_e}{\frac{d\mu_e}{ds}} \right)^2 \right] - \frac{\bar{w} a^2}{2D} \left(\frac{r_{0j}'}{r_{0j}} \right)^2 \left[\frac{2\mu_e}{\frac{d\mu_e}{ds}} \frac{r_{0j}'}{r_{0j}} - 2 - \left(\frac{\mu_e}{\frac{d\mu_e}{ds}} \right)^2 \right], \quad (3.33)$$

and

$$Y_6 = \frac{\bar{w} a}{D} \frac{r_{0j}'}{r_{0j}} \left[1 - \frac{r_{0j}'}{r_{0j}} \frac{\mu_e}{\frac{d\mu_e}{ds}} + \left(\frac{\mu_e}{\frac{d\mu_e}{ds}} \right)^2 \right] + \frac{3\mu_e}{D \left(\frac{d\mu_e}{ds} \right)^2}. \quad (3.34)$$

Also,

$$A_1 = D(W_6) \left(\frac{a^2}{252} - \frac{a}{105} - \frac{4}{35} \right) - D(W_5), \quad (3.35)$$

$$A_2 = - \left[\frac{\frac{d\mu_e}{ds}}{\mu_e} \right] \left[\frac{D(a-8)}{20} + 2D \left(-\frac{a^2}{252} + \frac{a}{105} + \frac{4}{35} \right) \right] - \left[\frac{r_{0j}'}{r_{0j}} \right] \left[D \left(-\frac{a^2}{252} + \frac{a}{105} + \frac{4}{35} \right) + \frac{\bar{w}}{35} (3a^2 - 4a + 48) \right] + \frac{a}{\mu_e D} - \left[\left(-\frac{a^2}{252} + \frac{a}{105} + \frac{4}{35} \right) \right] \left[\frac{D}{2} \frac{1}{\frac{d\mu_e}{ds}} + \frac{\bar{w} a^2}{2D} \frac{r_{0j}'}{r_{0j}} \left(1 - \frac{r_{0j}'}{r_{0j}} \frac{\mu_e}{\frac{d\mu_e}{ds}} \right) \right], \quad (3.36)$$

$$A_3 = [D(W_5)] \left[\frac{D}{2} \frac{\mu_e}{\frac{d\mu_e}{ds}} + \frac{a}{2} (X_5) \right] - \left[\left(3 + \bar{w} a \mu_e \frac{r_{0j}'}{r_{0j}} \right) \left(\frac{1}{D \frac{d\mu_e}{ds}} \right) \right] [-D(W_3)], \quad (3.37)$$

$$A_4 = [-\bar{\theta} a \mu_e] - [\bar{\theta} \mu_e a^2] [W_6], \quad (3.38)$$

$$A_5 = [\bar{\theta} \mu_e a^2 (X_8)] + [\bar{\theta} \mu_e a] \left[-\frac{a^2}{252} + \frac{a}{105} + \frac{4}{35} \right], \quad (3.39)$$

$$A_6 = \left[\frac{\bar{\theta} \mu_e a^2}{D} \right] \left[\frac{\bar{w} a^2}{2D} \frac{r_{0j}'}{r_{0j}} \left(1 - \frac{r_{0j}'}{r_{0j}} \frac{\mu_e}{\frac{d\mu_e}{ds}} \right) + \frac{D \mu_e}{2} \frac{1}{\frac{d\mu_e}{ds}} \right]$$

$$-\left[12-6a+(\bar{\theta}-\bar{w})a^2 u_e \frac{r_{0j}^{i'}}{r_{0j}} + (\bar{\theta}a^2 + D^2) \frac{du_e}{ds}\right], \quad (3.40)$$

$$A7 = \left[12-6a+(\bar{\theta}-\bar{w})a^2 u_e \frac{r_{0j}^{i'}}{r_{0j}} + (\bar{\theta}a^2 + D^2) \frac{du_e}{ds}\right] \left[-\frac{a^2}{252} + \frac{a}{105} + \frac{4}{35}\right] + \left[\frac{\bar{\theta}u_e a^2}{D}\right] \left[-D(W3)\right], \quad (3.41)$$

and

$$A8 = \left[12-6a+(\bar{\theta}-\bar{w})a^2 u_e \frac{r_{0j}^{i'}}{r_{0j}} + (\bar{\theta}a^2 + D^2) \frac{du_e}{ds}\right] \left[-\frac{(W6)}{D}\right] + \left[\bar{\theta}a u_e\right] \left[-\frac{(W4)}{D}\right]. \quad (3.42)$$

Equations (1.43) and (3.11) can now be solved simultaneously for $\frac{da}{ds}$ and $\frac{dD}{ds}$, as was done with equations (3.04) and (3.05), to yield:

$$\frac{da}{ds} = \frac{(R2)(R) - (A)(R3)}{(R2)(B) - (A)(R1)} \quad (3.43)$$

and

$$\frac{dD}{ds} = \frac{(R1)(R) - (B)(R3)}{(R1)(A) - (B)(R2)}. \quad (3.44)$$

where,

$$A = \left(-\frac{a^2}{252} + \frac{a}{105} + \frac{4}{35}\right) - \frac{2\bar{\theta}}{35D^2} (3a^2 - 4a + 48), \quad (3.45)$$

$$B = D \left(-\frac{a}{126} + \frac{1}{105}\right) + \frac{2\bar{\theta}}{35D} (6a-4), \quad (3.46)$$

and

$$\begin{aligned} R = & -\left[\frac{d\bar{u}_e}{d\bar{s}}\right]\left[\frac{D}{20}(8-a) + 2D\left(-\frac{a^2}{252} + \frac{a}{105} + \frac{4}{35}\right)\right. \\ & \left. + \frac{4\bar{\Theta}}{35D}(3a^2 - 4a + 48)\right] - \frac{d}{d\bar{s}}(\ln r_0^j)\left[D\left(-\frac{a^2}{252} + \frac{a}{105} + \frac{4}{35}\right)\right. \\ & \left. + \frac{\bar{\omega}}{35D}(3a^2 - 4a + 48)\right] + \frac{a}{u_e D} . \end{aligned} \quad (3.47)$$

4. Application of the Governing Equations to Problems of
Second-Order Flow Past a Circular Cylinder
and Second-Order Flow Past a Sphere

This section describes the application of equations (3.43) and (3.44) to the problems of second-order flow past a circular cylinder and second-order flow past a sphere.

The values of $\alpha(0)$ and $D(0)$, the stagnation-point values, have already been determined in Section 2 of this chapter and can be found in Tables A and B. If we use a small step size ($\Delta S = 0.001$), we can approximate the integration from one step to the next by

$$\alpha_{n+1} = \alpha_n + \left(\frac{d\alpha}{ds} \right)_n (\Delta S) , \quad (4.01)$$

and

$$D_{n+1} = D_n + \left(\frac{dD}{ds} \right)_n (\Delta S) , \quad (4.02)$$

and thus determine the value of α and D at each step along the body contour.

To determine $\frac{d\alpha}{ds}$ and $\frac{dD}{ds}$ at the stagnation point we can expand α and D , about the stagnation point, in the form

$$\alpha = \alpha_1 + \alpha_2 s^2 + \dots , \quad (4.03)$$

and

$$D = D_1 + D_2 s^2 + \dots , \quad (4.04)$$

to obtain,

$$\left(\frac{da}{ds}\right)_0 = 0 , \quad (4.05)$$

and

$$\left(\frac{dD}{ds}\right)_0 = 0 . \quad (4.06)$$

For $\eta \geq 1$ (4.01 and 4.02), equations (3.43) and (3.44) should be used to calculate $\frac{da}{ds}$ and $\frac{dD}{ds}$, respectively.

There is no assurance that the boundary layer equations used to develop the momentum integral relation are valid near separation. Therefore, calculations should not be carried past the point of separation. Separation is defined to occur when the shear stress on the body surface vanishes.

To use (3.43) and (3.44) for calculations, the following terms appearing in these equations will be defined.

For the circular cylinder:

$$\mu_e = 2 \sin(s) , \quad (4.07)$$

$$r_0^j = 1 , \quad (4.08)$$

and

$$r_0^{j'} = 0 . \quad (4.09)$$

For the sphere:

$$\mu_e = \frac{3}{2} \sin(s) , \quad (4.10)$$

$$r_0^j = s , \quad (4.11)$$

and

$$r_0^{j'} = 1 \quad . \quad (4.12)$$

It should be noted that (4.07) and (4.10) assume that the potential solution is correct. The approximation involved here is commonly used for flow problems of this type. Actually, behind bodies such as cylinders and spheres, there exists a region of strongly decelerated flow (so-called wake). In this region, the pressure distribution deviates considerably from that of the frictionless fluid and in fact, the upstream solution is affected.

With α and D known along the body contour, it will be of interest to calculate:

δ^* - given by equation (1.38),

θ^* - given by equation (1.39),

ζ^* - given by equation (1.40),

ζ_w - given by equation (1.41),

and

$$\text{Viscous Drag} = 2 \int_0^{\text{separation}} \zeta_w \cdot \sin(s) ds$$

A computer program, written to calculate the variables described above, is included as Appendix B. This program is for second-order flow past a circular cylinder. To use it for second-order flow past a sphere, (4.10), (4.11) and (4.12) should replace (4.07), (4.08) and (4.09); and stagnation values for α and D from Table B should replace those from Table A.

5. Discussion of Results

Values of α , D and $f''(0)$ for plane and axisymmetric stagnation-point flows are presented in Tables A and B. These results are also shown in Figures 2 and 3.

Figure 4 shows a comparison of solutions obtained by the approximate method and an exact method. The approximate curve, obtained from the fourth-degree polynomial and appropriate boundary conditions, is almost identical to that obtained by Pohlhausen [11]. The exact solution shown in Figure 4 was obtained from a Newtonian finite-difference solution programmed by R. E. Whitehead.

Figures 5 and 6 show the effect of increases in $\bar{\Theta}$ for flow past a circular cylinder. An interesting result is shown for the wall shear stress (Figure 5); there is a gradual increase and then a slight decrease of the second-order wall shear stress from that of the Newtonian fluid for positive $\bar{\Theta}$.

Figure 7 shows the effect of small increases in $\bar{\Theta}$ on the velocity profile for flow past a circular cylinder. These curves are typical of those for flow past a sphere with positive $\bar{\Theta}$. The effect of changes in $\bar{\omega}$ on the velocity profile was slight and is not shown.

Figures 8, 9, 10, 11 and 12 show the effect of the second-order viscosity terms on flow past a sphere. Changes in $\bar{\omega}$ either

raise or lower the values from those of Newtonian flow, but changes in $\bar{\Theta}$ cause an increase and decrease in values from Newtonian flow and the second-order and Newtonian curves cross.

Figure 13 shows that positive increases in $\bar{\Theta}$ and $\bar{\omega}$ cause a linear increase in the viscous drag on the circular cylinder and sphere. The result of a decrease in $\bar{\omega}$ from the Newtonian case, however, is a reduction in viscous drag. From this trend we may conclude that a substantial reduction in viscous drag may occur experimentally, when a second-order fluid, with large negative values of $\bar{\omega}$, is substituted for a Newtonian fluid. Figure 14 shows the effect of changes in the second-order terms on the location of the point of separation.

The constitutive equation for a second-order liquid is valid for small values of Θ and ω . Within this range of Θ and ω the results should vary linearly. The approximate method has shown that the allowable range for Θ and ω is much smaller than might be expected. For values of $\bar{\Theta} \cong 0.06$ the results were highly non-linear. It thus appears that the use of this constitutive equation is limited to an extremely small range of Θ and ω .

TABLE A

Numerical Results for Plane Stagnation-Point Flows

j	$\bar{\theta}$	$\bar{\omega}$	α	D	$F''(0)$	Exact $F''(0)$
0	0.00	-	3.1754	1.8778	1.1957	1.233
0	0.01	-	3.1240	1.8095	1.2208	
0	0.02	-	3.0743	1.7418	1.2481	
0	0.03	-	3.0259	1.6742	1.2780	
0	0.04	-	2.9787	1.6066	1.3110	
0	0.05	-	2.9323	1.5385	1.3477	
0	0.06	-	2.8868	1.4698	1.3888	
0	0.07	-	2.8418	1.4000	1.4353	
0	0.08	-	2.7973	1.3289	1.4884	
0	0.09	-	2.7533	1.2560	1.5500	
0	0.10	-	2.7096	1.1809	1.6224	1.350
0	0.11	-	2.6661	1.1029	1.7093	
0	0.12	-	2.6228	1.0213	1.8160	
0	0.13	-	2.5797	0.9348	1.9512	
0	0.14	-	2.5366	0.8420	2.1301	
0	0.15	-	2.4936	0.7403	2.3818	
0	0.16	-	2.4505	0.6251	2.7719	
0	0.17	-	2.4074	0.4869	3.4965	
0	0.18	-	2.3643	0.2944	5.6794	

TABLE B

Numerical Results for Axisymmetric Stagnation-Point Flows

j	$\bar{\theta}$	$\bar{\omega}$	α	D	$F''(0)$	Exact $F''(0)$	10
1	0.00	-0.10	3.5922	2.2535	1.3015		
1	0.00	-0.05	3.0572	1.9394	1.2871		
1	0.00	0.00	2.7860	1.7731	1.2829	1.312	
1	0.00	0.05	2.5939	1.6468	1.2861		
1	0.00	0.10	2.4435	1.5398	1.2957		
1	0.00	0.15	2.3193	1.4436	1.3118		
1	0.00	0.20	2.2133	1.3539	1.3348		
1	0.05	-0.05	3.2653	1.8606	1.4329		
1	0.05	0.00	2.8820	1.6424	1.4327	1.463	
1	0.05	0.05	2.6461	1.4947	1.4454		
1	0.05	0.10	2.4714	1.3732	1.4695		
1	0.05	0.15	2.3319	1.2647	1.5055		
1	0.05	0.20	2.2154	1.1629	1.5555		
1	0.10	0.00	3.0260	1.5075	1.6389		
1	0.10	0.05	2.7158	1.3254	1.6730		
1	0.10	0.10	2.5069	1.1828	1.7305		
1	0.10	0.15	2.3474	1.0554	1.8159		
1	0.10	0.20	2.2178	0.9334	1.9400		
1	0.15	0.00	3.2897	1.3828	1.9425		
1	0.15	0.05	2.8156	1.1316	2.0316		
1	0.15	0.10	2.5534	0.9537	2.1860		
1	0.15	0.15	2.3668	0.7917	2.4409		
1	0.15	0.20	2.2208	0.6245	2.9037		
1	0.16	0.00	3.3797	1.3651	2.0214		
1	0.16	0.10	2.5645	0.9007	2.3248		
1	0.01	-0.01	2.8508	1.7774	1.3096		

TABLE B (Cont'd)

Numerical Results for Axisymmetric Stagnation-Point Flows

j	$\bar{\theta}$	$\bar{\omega}$	α	D	$f''(0)$	Exact $f''(0)$	10
1	0.01	-0.02	2.9027	1.8093	1.3099		
1	0.04	-0.08	3.6640	2.1232	1.4090		
1	0.04	-0.04	3.1235	1.8229	1.3990		
1	0.06	-0.06	3.4750	1.9304	1.4698		

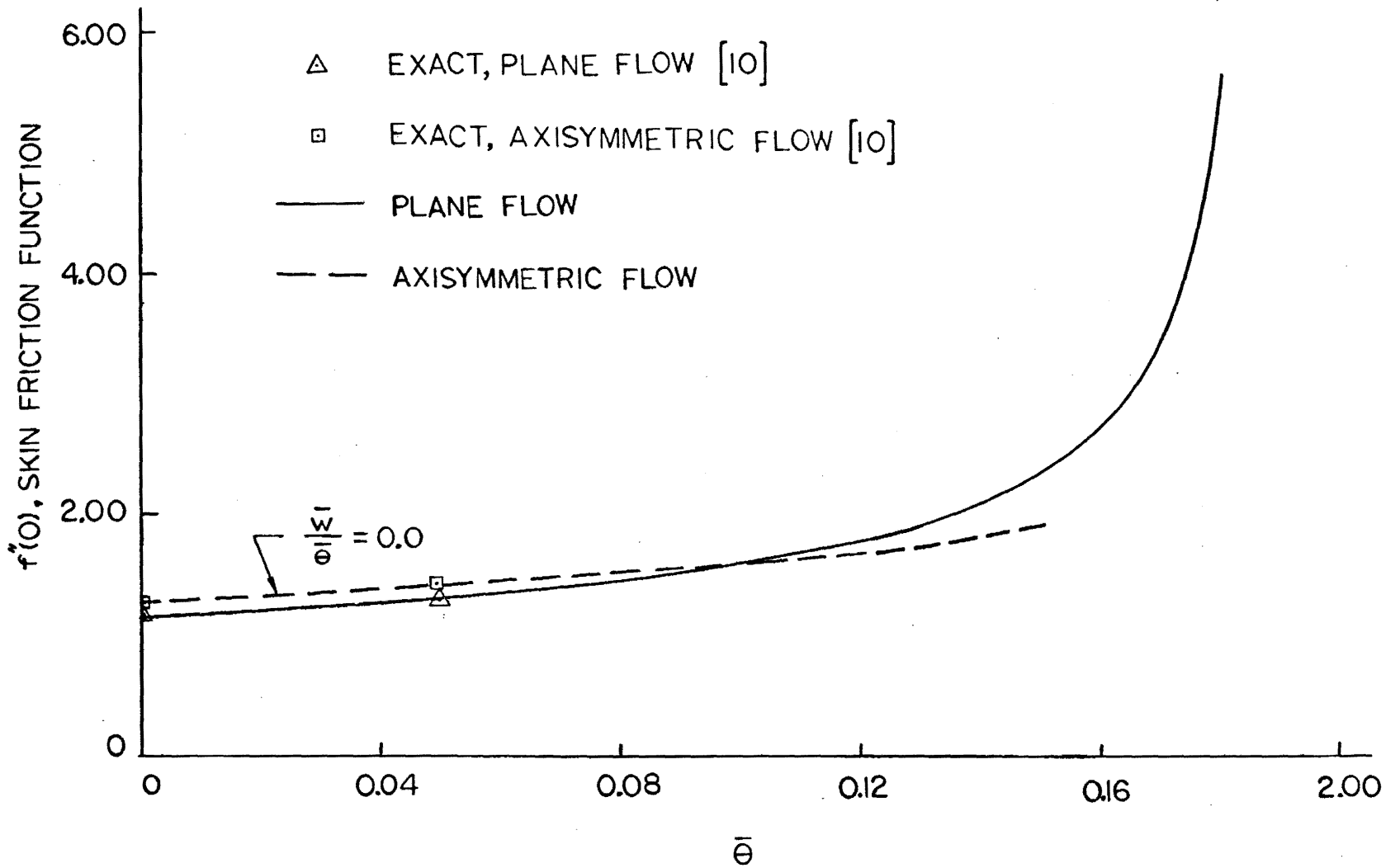


Figure 2 - Stagnation-Point Skin Friction Variation with $\bar{\theta}$ and $\bar{\omega}$

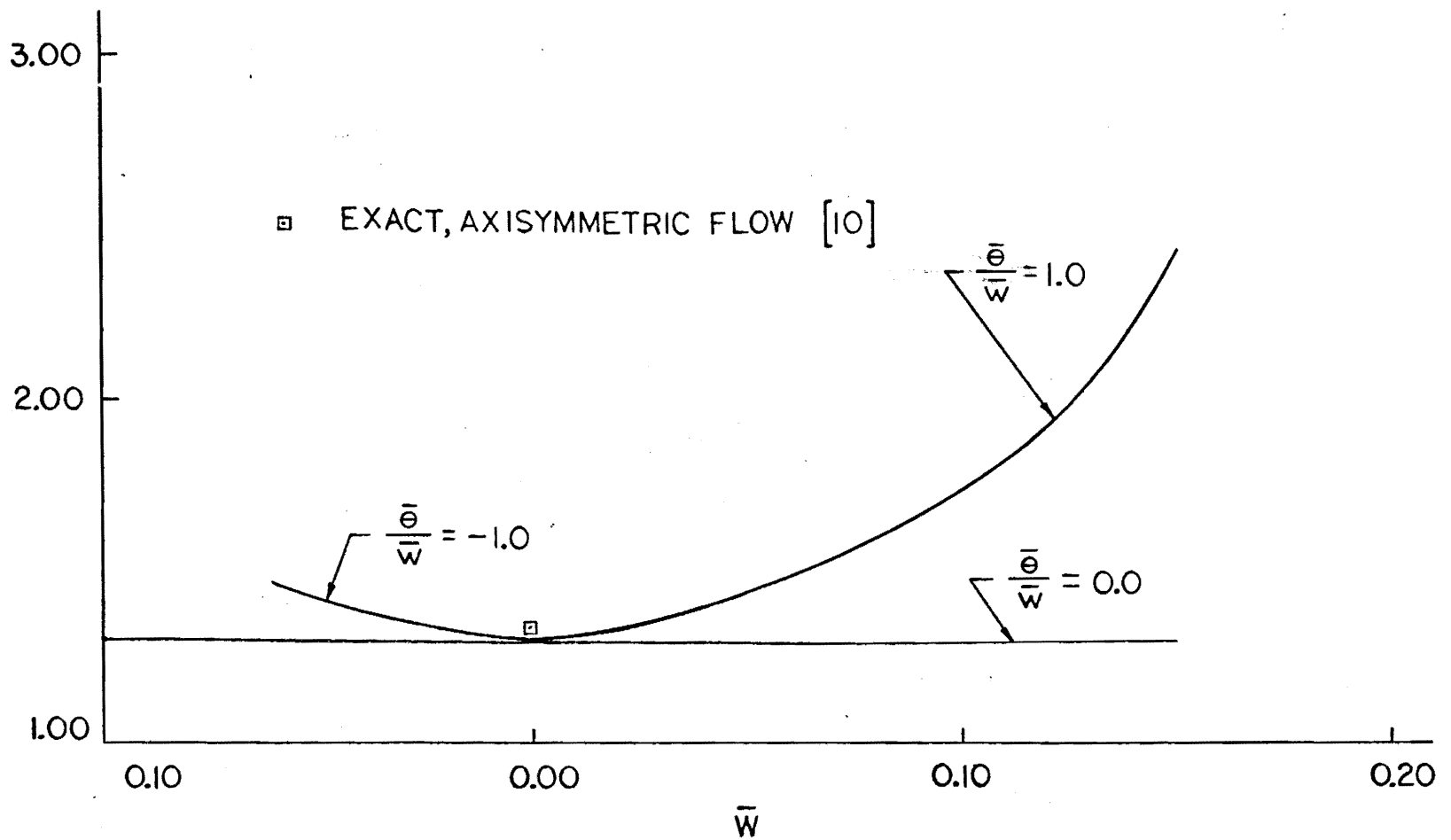


Figure 3 - Axisymmetric Stagnation-Point Skin Friction Variation with $\bar{\theta}$ and $\bar{\omega}$

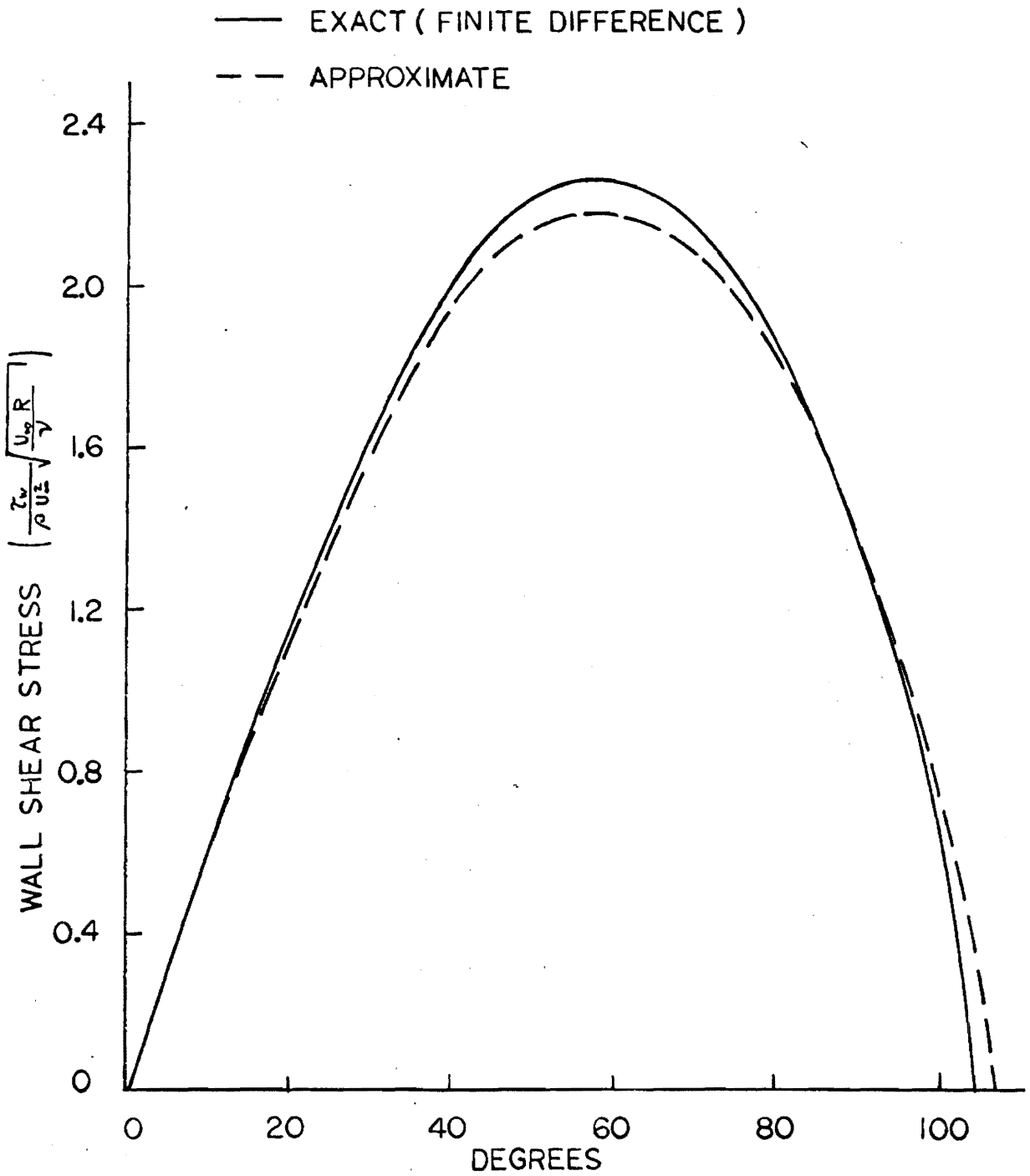


Figure 4 - Comparison of Exact and Approximate Wall Shear Stress for Newtonian Flow Past a Circular Cylinder.

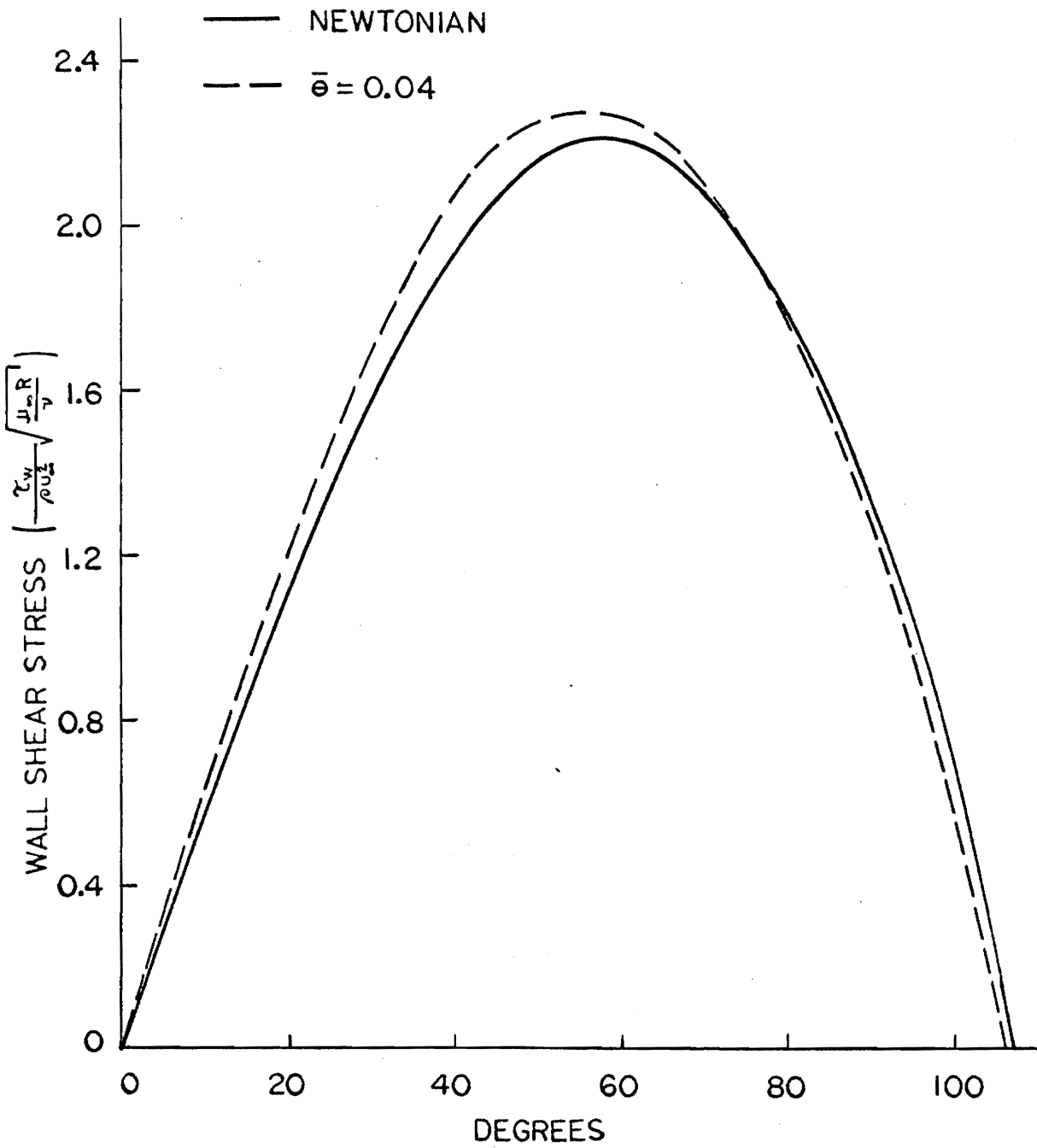


Figure 5 - Comparison of Wall Shear Stress for Newtonian and Second-Order Flow Past a Circular Cylinder

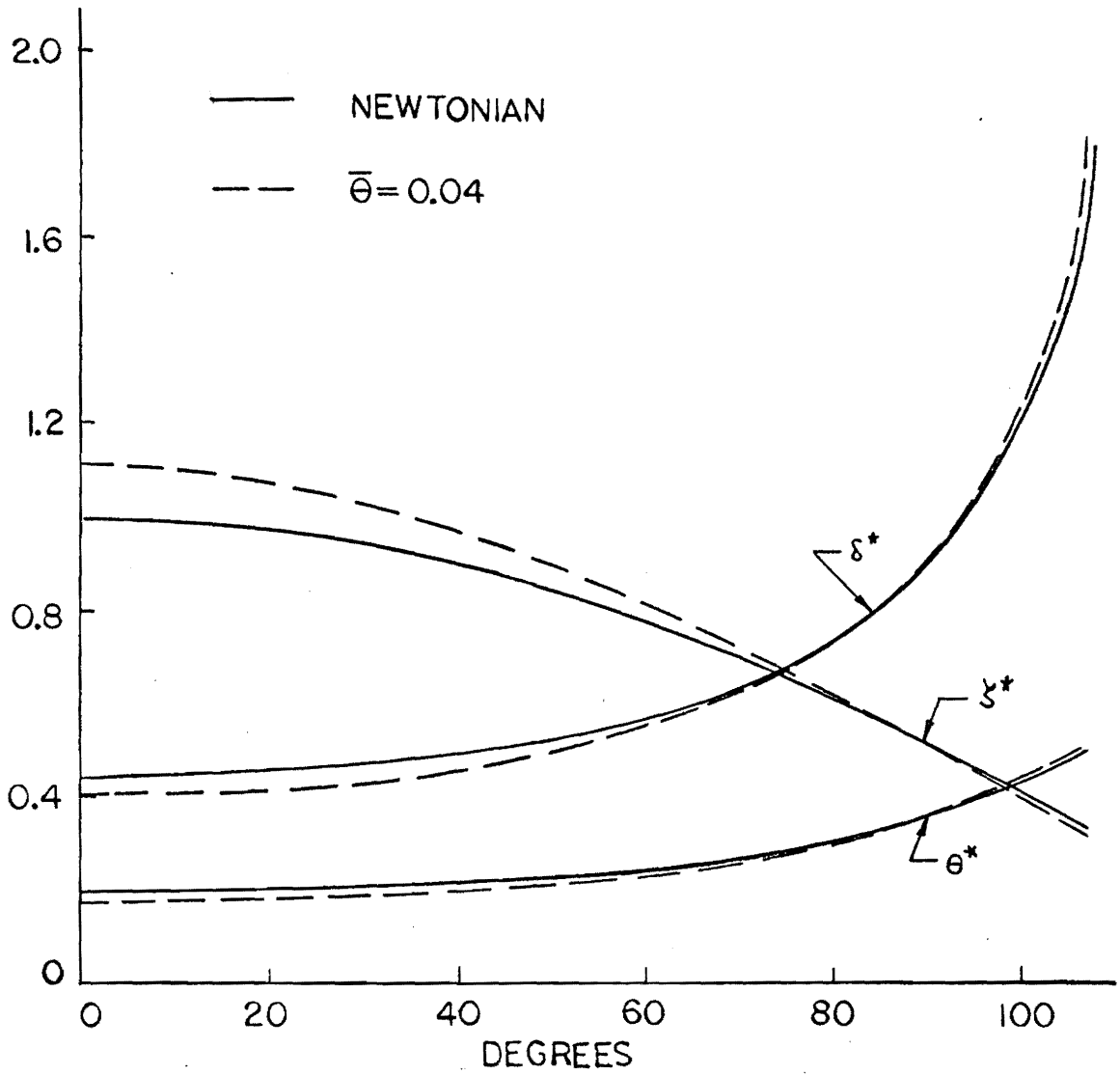


Figure 6 - Comparison of Boundary-Layer Thickness for Newtonian and Second-Order Flow Past a Circular Cylinder

— NEWTONIAN

- - - $\bar{\theta} = 0.04$

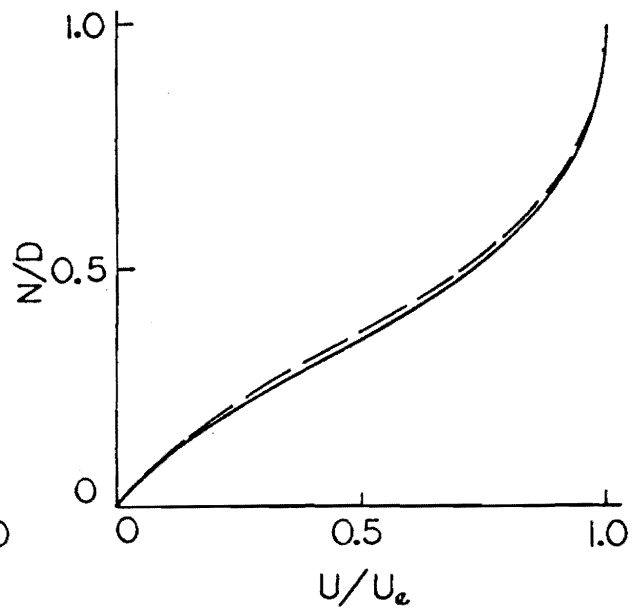
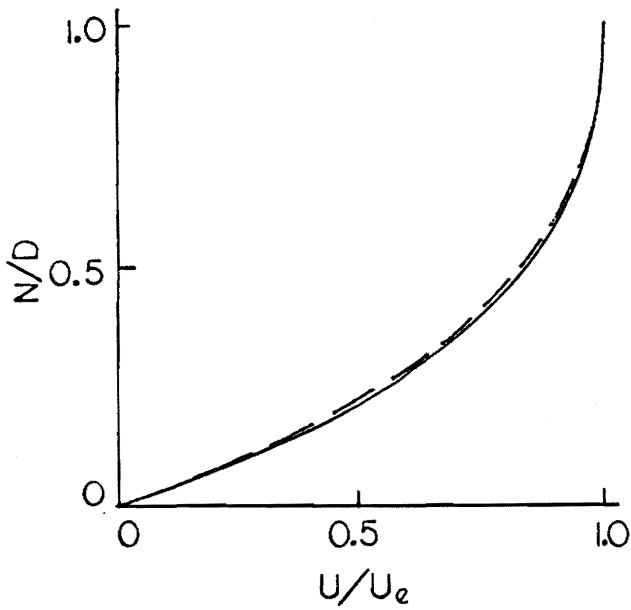
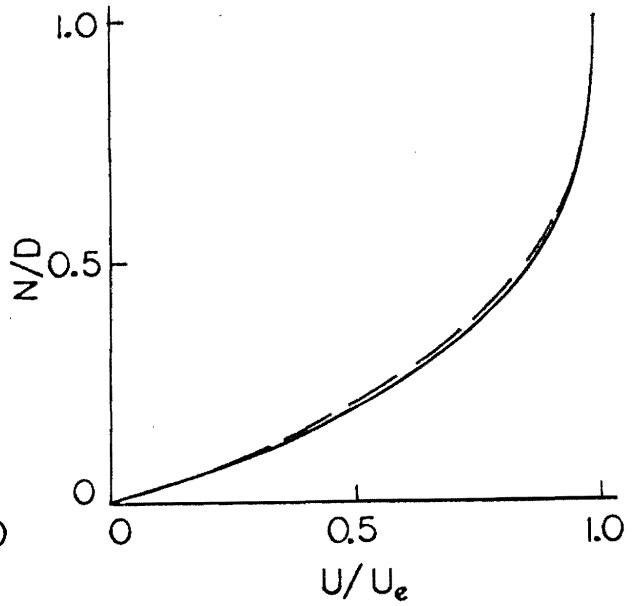
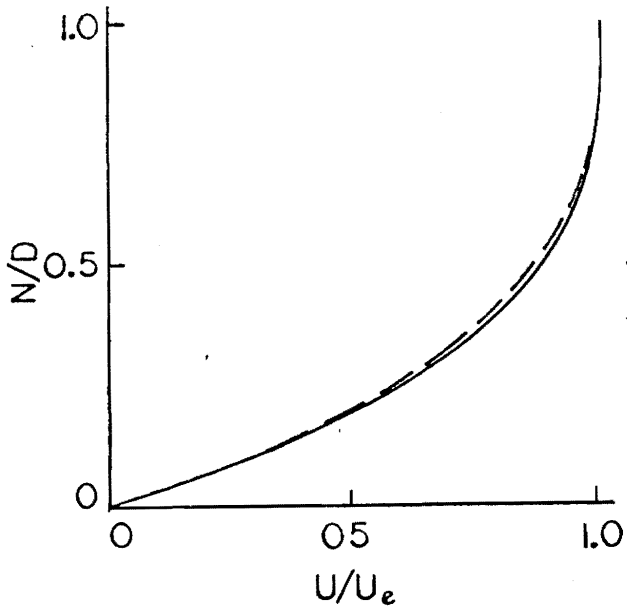


Figure 7 - Comparison of Velocity Profiles for Newtonian and Second-Order Flow Past a Circular Cylinder

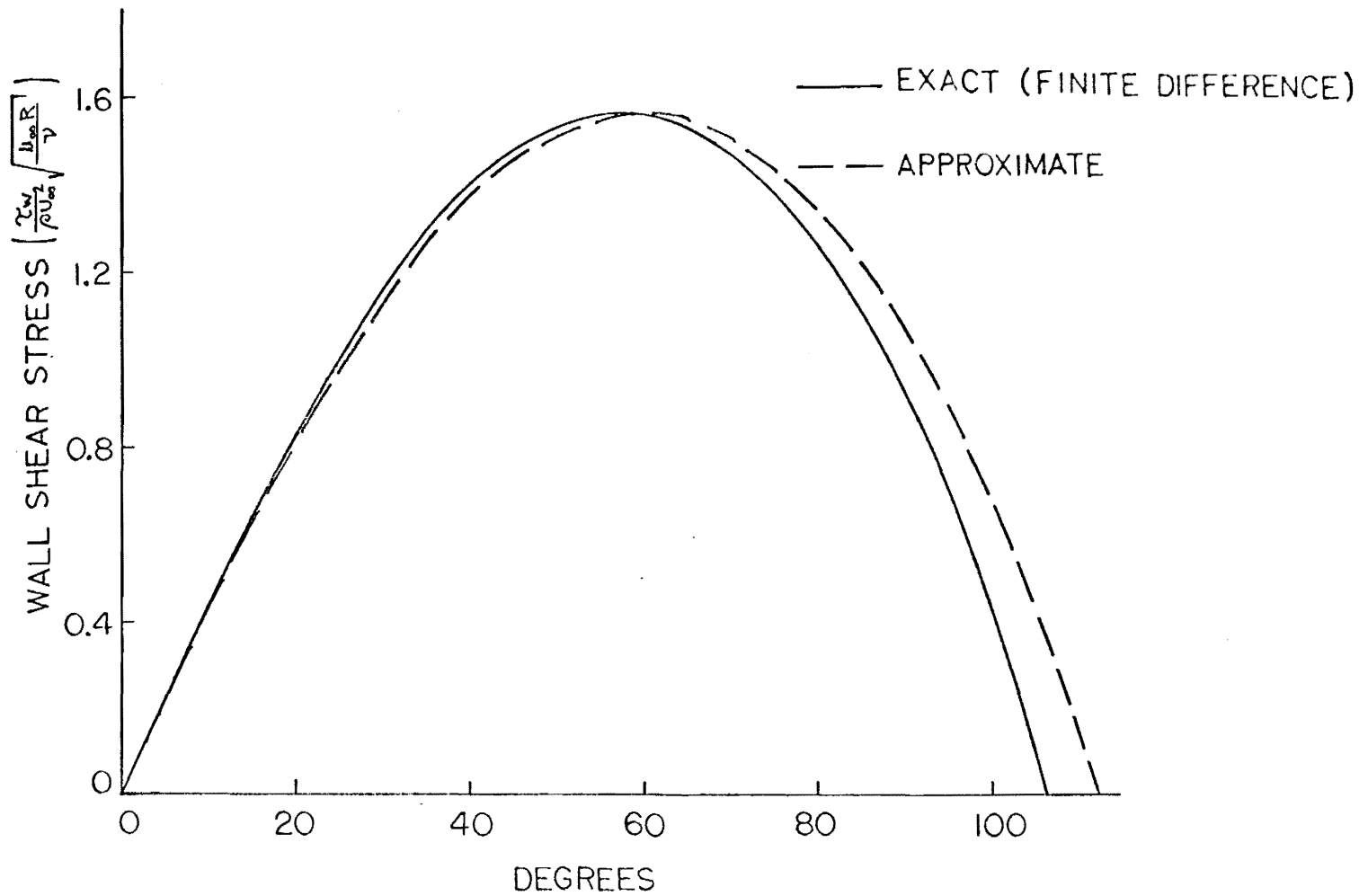


Figure 8 - Comparison of Wall Shear Stress for Newtonian and Second-Order Flow Past a Sphere

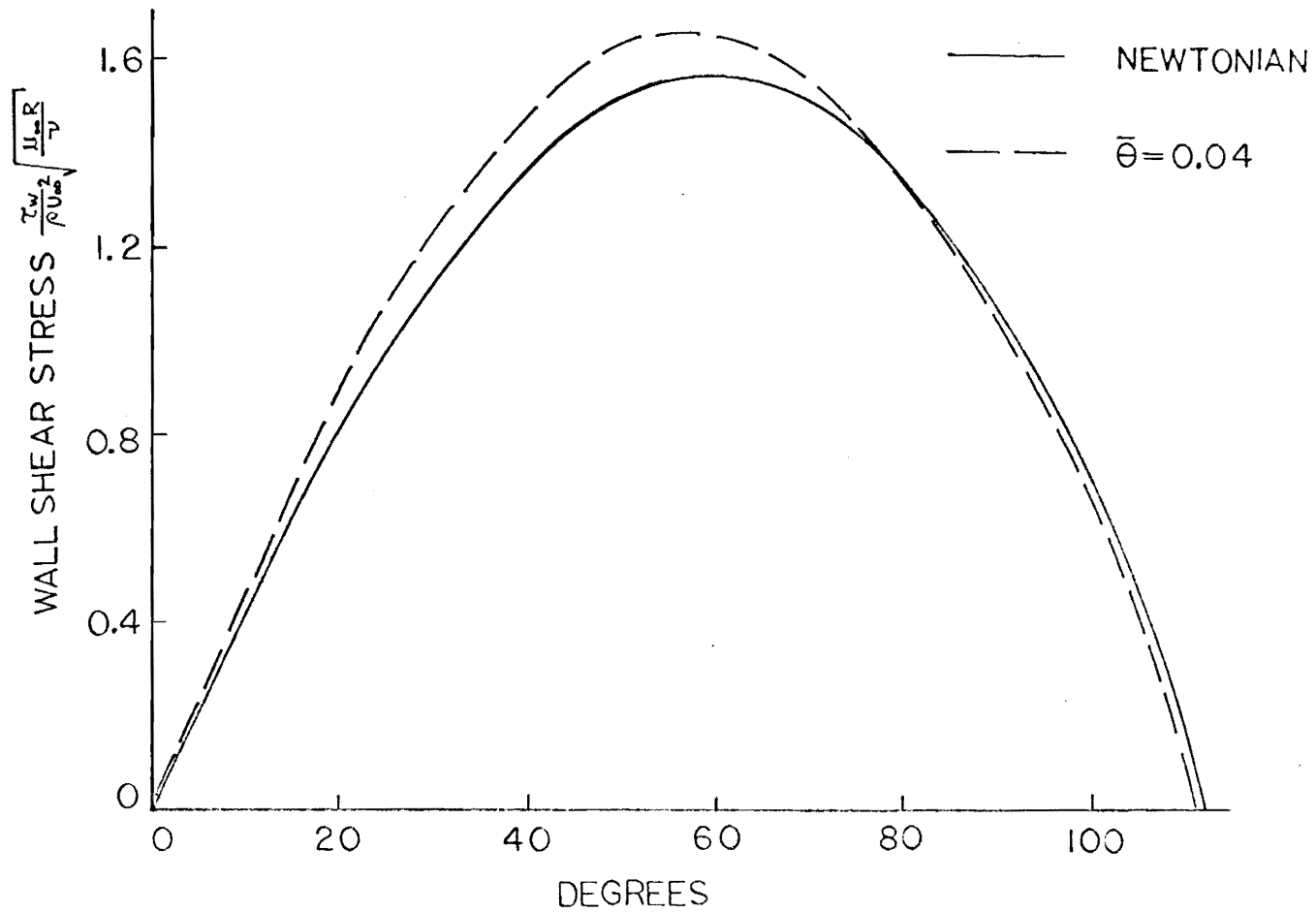


Figure 9 - Comparison of Wall Shear Stresses for Newtonian and Second-Order Flow Past a Sphere with $\bar{w} = 0.00$

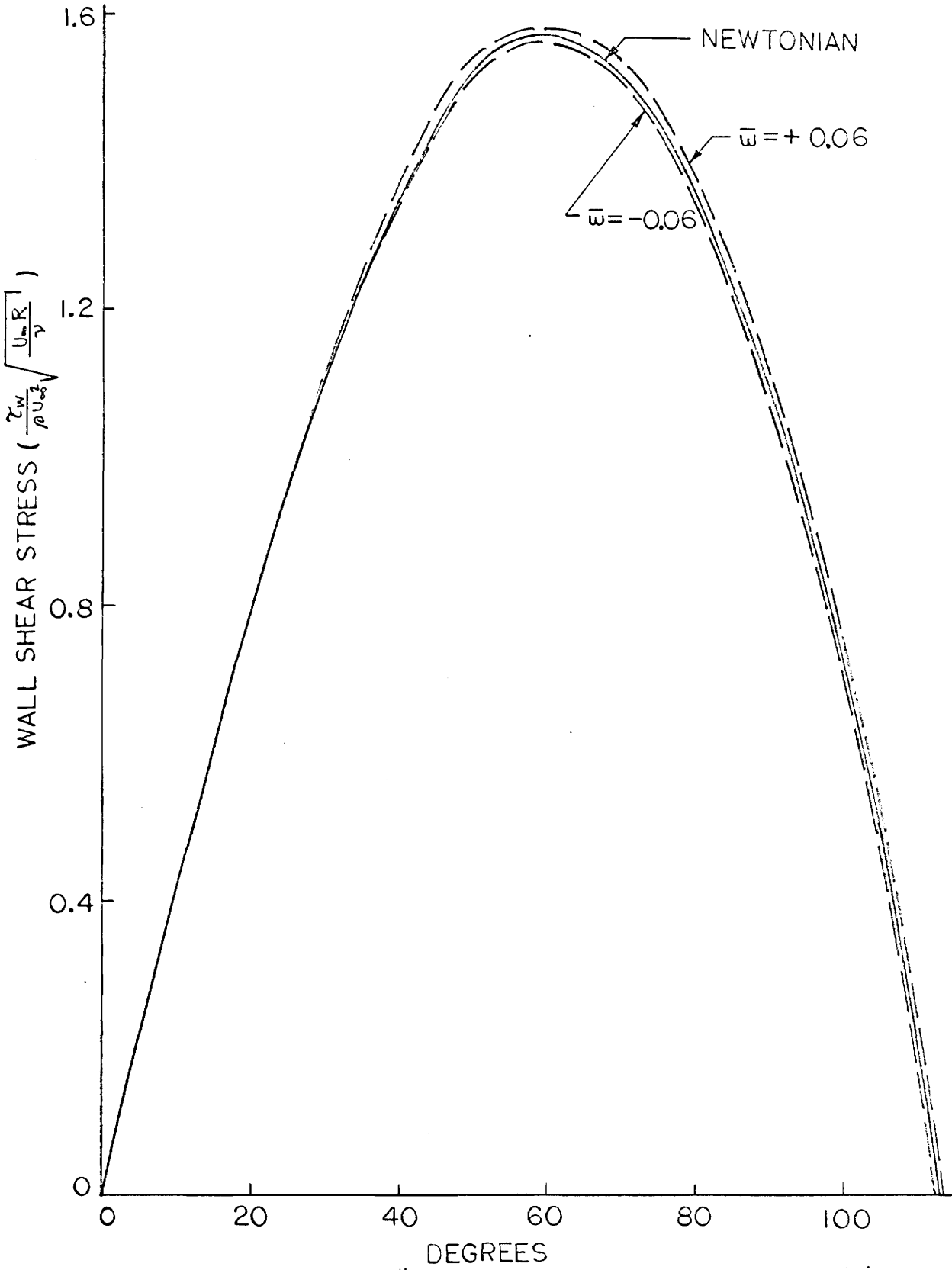


Figure 10 - Comparison of Wall Shear Stress for Newtonian and Second-Order Flow Past a Sphere with $\bar{\omega} = 0.00$

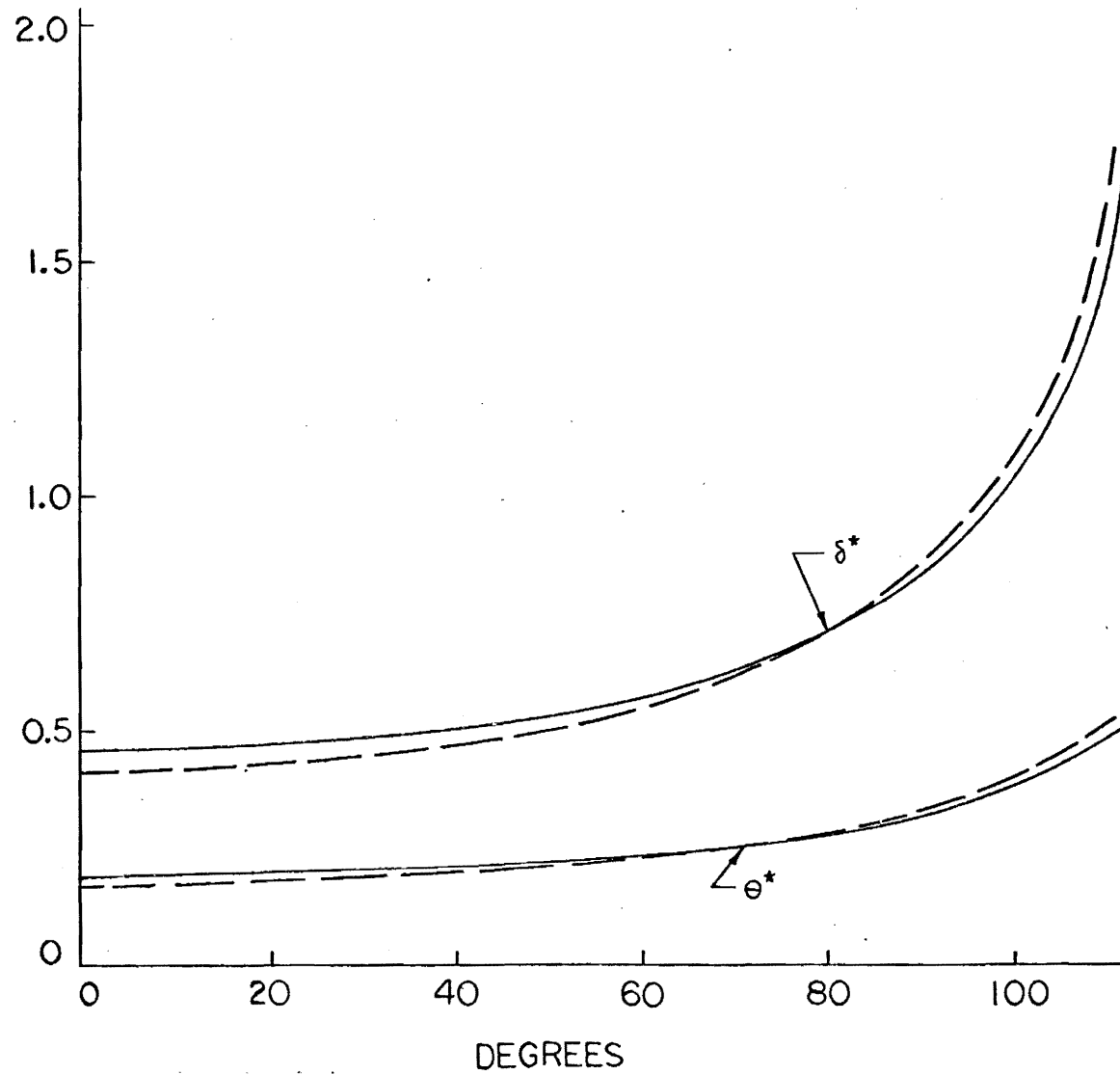


Figure 11 - Comparison of Boundary-Layer Thicknesses for Newtonian and Second-Order Flow Past a Sphere with $\bar{\omega} = 0.00$

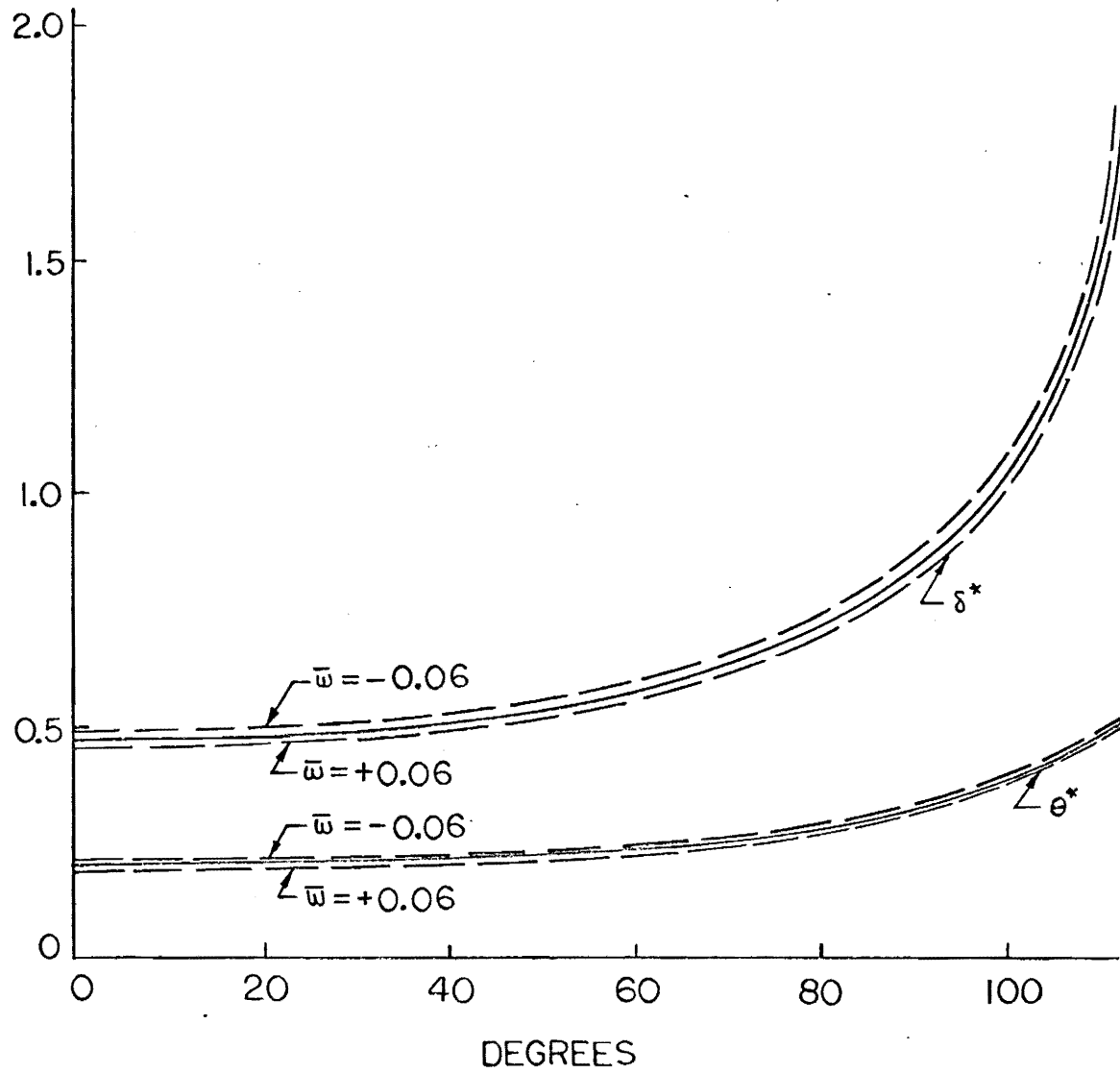
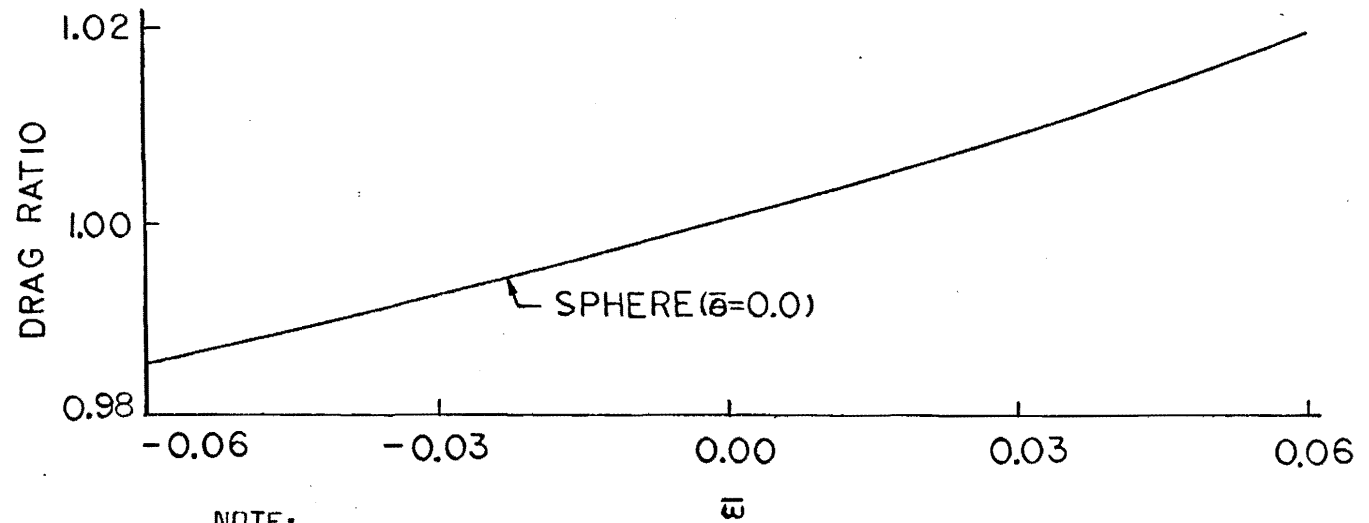
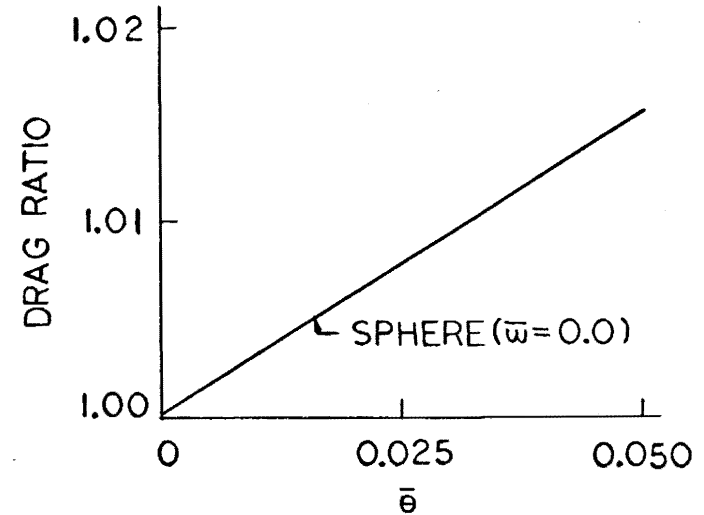
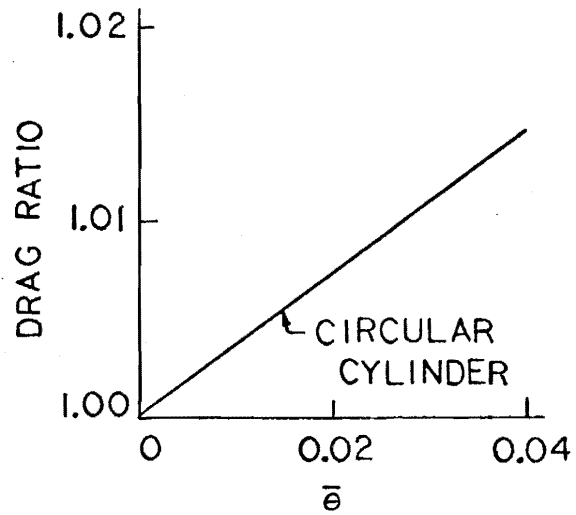


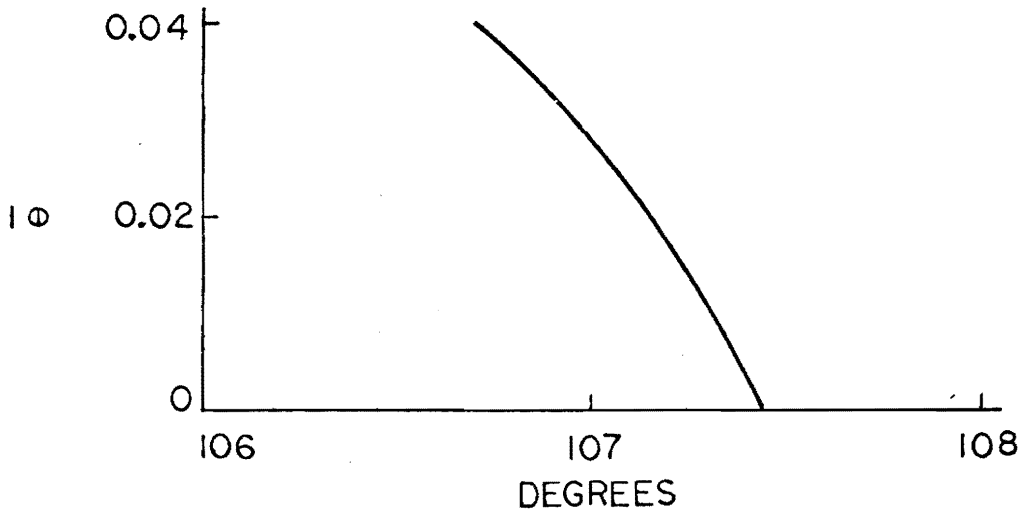
Figure 12 - Comparison of Boundary-Layer Thicknesses for Newtonian and Second-Order Flow Past a Sphere with $\bar{\omega} = 0.00$



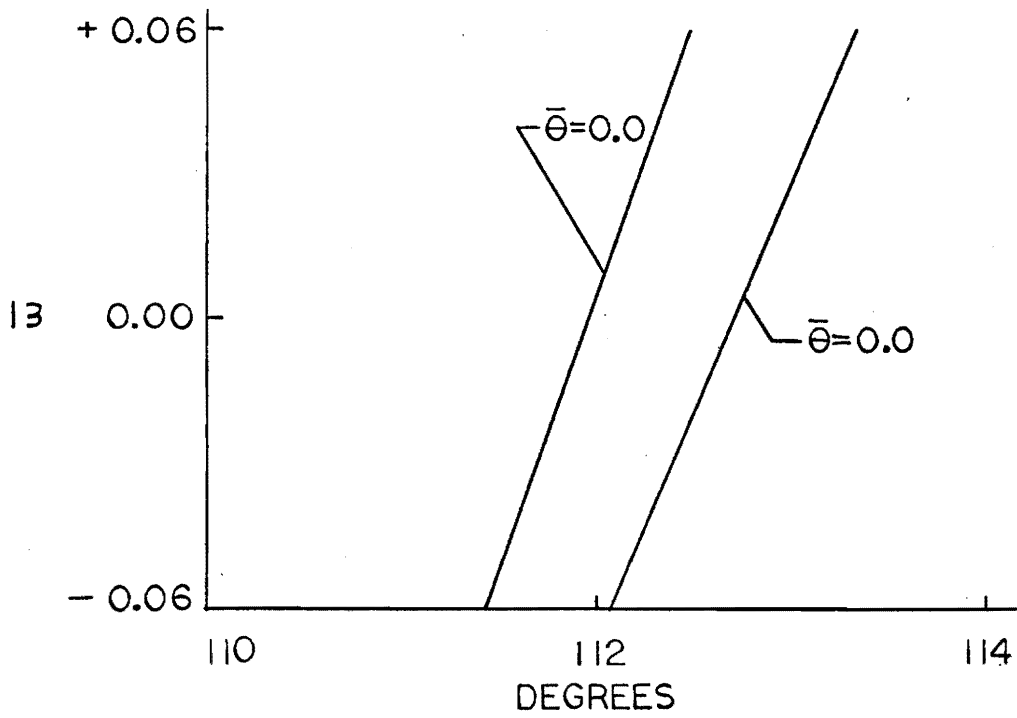
NOTE:

Drag Ratio = Viscous Drag/Viscous Drag for Newtonian Flow

Figure 13 - Drag Ratios for Flow Past a Sphere and Flow Past a Circular Cylinder



FLOW PAST A CIRCULAR CYLINDER



FLOW PAST A SPHERE

Figure 14 - Comparison of Separation Points for Newtonian and Second-Order Flows

IX. LIST OF REFERENCES

1. Acrivos, A., Shah, M. J. and Petersen, E. E., "Momentum and Heat Transfer in Laminar Boundary-Layer Flows of Non-Newtonian Fluids Past External Surfaces," AICHE J., 6, 2, 312 - 317, June, 1960.
2. Kapur, J. N. and Srivastava, R. C., "Similar Solutions of the Boundary Layer Equations for Power Law Fluids," ZAMP, 14, 25, 383 - 389, 1963.
3. Reiner, M., "A Mathematical Theory of Dilatancy," M. Amer. J. Math., 67, 350 - 362, 1945.
4. Nanda, R. S., "On the Three-Dimensional Flow of Certain Non-Newtonian Liquids," Applied Scientific Research [A], 11, 376 - 386, 1962 - 63.
5. Srivastava, A. C., "The Flow of a Non-Newtonian Liquid Near a Stagnation Point," ZAMP, 9, 6, 80 - 84, 1958.
6. Datta, S., "Slow Steady Rotation of a Sphere in a Non-Newtonian Inelastic Viscous Fluid," Applied Scientific Research [A], 11, 47 - 52, 1962 - 63.

7. Rajeswari, G. K., "Laminar Boundary Layer on Rotating Sphere and Spheroids in Non-Newtonian Fluids," ZAMP, 13, 5, 442 - 459, 1962.
8. Coleman, B. D. and Noll, W., "An Approximate Theorem for Functionals, with Applications in Continuum Mechanics," Archive for Rational Mechanics and Analysis, 6, 5, 335 - 370, 1960.
9. Markovitz, H. and Coleman, B. D., "Incompressible Second-Order Fluids," Advances in Applied Mechanics, 8, Academic Press, New York, 69 - 101, 1964.
10. Davis, R. T., "Boundary-Layer Theory for Viscoelastic Liquids," To be presented at the 10th Midwestern Mechanics Conference, Fort Collins, Colorado, August 21 - 23, 1967.
11. Pohlhausen, K., "Zur näherungsweise Integration der Differentialgleichung der laminaren Reibungsschicht," ZAMM, 1, 252, 1921.

X. ACKNOWLEDGEMENTS

The author wishes to express his appreciation to his advisor, Professor D. T. Mook, for his contributions both during the preparation of this thesis and in the classroom.

Also to Professor R. T. Davis, who suggested this area of investigation and spent many hours with the author in patient discussion concerning the content of this thesis.

Also to Professor C. W. Smith for his guidance and suggestions, and to Professor D. H. Pletta for his help in obtaining a NASA Fellowship to finance graduate study.

Last, but certainly not least, to Terry for her patience and understanding.

The vita has been removed
from the scanned document

APPENDIX A

The following program, written in FORTRAN IV for the I.B.M. 7040 Digital Computer, was used to find solutions for the stagnation-point flows presented in Tables A and B.

The input data required for this program is:

- CUT - Acceptable error for value of Q ,
 calculated from (2.13)
- DOMGA - Increment for values of omega bar
- DTHTA - Increment for values of theta bar
- KM - Number of different values of
 theta bar
- KN - Number of different values of
 omega bar
- OMGA(1) - Initial value of omega bar
- THTA(1) - Initial value of theta bar
- U1 - Value of μ , in equation (2.13)
- XI, XF - Range of values for Q
- XJ - 0 for plane flow, 1 for axisymmetric
 flow

The output received from this program is:

- A - Stagnation-point value of Q
- D - Stagnation-point value of D
- F"(0) - Stagnation-point skin friction
 function

C COMPUTER PROGRAM TO CALCULATE THE STAGNATION VALUES
C AXISYMMETRIC FLOW

DIMENSION THTA(120), OMGA(120)

XI=2.450

XF=3.750

DX=0.50

CUT=0.00001

DOMGA=0.01

DTHTA=0.01

U1=1.50

XJ=1.0

KM=12

KN=16

OMGA(1)=-0.15

THTA(1)=0.00

DO 600 M=1,KM

DO 500 N=1,KN

WRITE (6,151)

151 FORMAT (1H /////55X22HVISCOSITY COEFFICIENTS//)

WRITE(6,152) THTA(M)

152 FORMAT (1H 58X10HTheta BAR=F5.2)

WRITE(6,153) OMGA(N)

153 FORMAT (1H 58X10HOMEGA BAR=F5.2)

WRITE(6,154)

154 FORMAT(1H //58X17HSTAGNATION VALUES////)

```
X=XI
Y1=6.*X-12.
Y2=-XJ*OMGA(N)+(1.+XJ)*THTA(M)
T=Y1-(X**2)*U1*Y2
Y3=(8.-X)/20.
Y4=(-X**2/252.+X/105.+4./35.)
V=Y3+(XJ+2.)*Y4
TV=T*V
Y5=3.*X**2-4.*X+48.
U=U1*((4.*THTA(M)+XJ*OMGA(N))/35.)*Y5-X
102 Y=TV+U
103 CONTINUE
    IF(ABS(Y)-CUT)104,104,106
104 B=((6.*X-12.)/U1-X**2*(-XJ*OMGA(N)+(1.+XJ)*THTA(M)))*
    1*0.50
    WRITE(6,155) X,B
155 FORMAT(48X,2HA=F8.4,16X2HD=F8.4)
    SFF=(X/B)/SQRT(U1)
    WRITE(6,157) SFF
157 FORMAT(//50X,23HSKIN FRICTION FUNCTION=F7.4//)
106 D=X
    E=Y
    X=X+DX
    Y1=6.*X-12.
    Y2=-XJ*OMGA(N)+(1.+XJ)*THTA(M)
```

$$T=Y1-(X**2)*U1*Y2$$

$$Y3=(8.-X)/20.$$

$$Y4=(-X**2/252.+X/105.+4./35.)$$

$$V=Y3+(XJ+2.)*Y4$$

$$TV=T*V$$

$$Y5=3.*X**2-4.*X+48.$$

$$U=U1*((4.*THTA(M)+XJ*OMGA(N))/35.)*Y5-X$$

$$Y=TV+U$$

107 IF(Y)108,103,109

108 IF(E)111,106,110

109 IF(E)110,106,111

110 VX=D+DX/10.

$$X=VX$$

$$Y1=6.*X-12.$$

$$Y2=-XJ*OMGA(N)+(1.+XJ)*THTA(M)$$

$$T=Y1-(X**2)*U1*Y2$$

$$Y3=(8.-X)/20.$$

$$Y4=(-X**2/252.+X/105.+4./35.)$$

$$V=Y3+(XJ+2.)*Y4$$

$$TV=T*V$$

$$Y5=3.*X**2-4.*X+48.$$

$$U=U1*((4.*THTA(M)+XJ*OMGA(N))/35.)*Y5-X$$

$$VX=X$$

$$VY=TV+U$$

1000 GO TO 112

```
111 IF(XF-X)1486,1486,1004
1004 DX=0.50
1005 GO TO 103
112 IF(ABS(VY)-CUT)113,113,115
113 X=VX
      B=((6.*X-12.)/U1-X**2*(-XJ*OMGA(N)+(1.+XJ)*THTA(M)))*
1*0.50
      WRITE(6,156) X,B
156 FORMAT(48X,2HA=F8.4,16X2HD=F8.4)
      SFF=(X/B)/SQRT(U1)
      WRITE(6,158) SFF
158 FORMAT(//50X,23HSKIN FRICTION FUNCTION=F7.4//)
1001 GO TO 111
115 IF (VY)116,1486,117
116 IF(E)118,1486,119
117 IF(E)119,1486,118
118 E=VY
      D=VX
1002 GO TO 110
119 Y=VY
      X=VX
      DX=DX/10.
1003 GO TO 110
1486 CONTINUE
      OMGA(N+1)=OMGA(N)+DOMGA
```


500 CONTINUE

THTA(M+1)=THTA(M)+DTHTA

600 CONTINUE

STOP

END

APPENDIX B

The following program, written in FORTRAN IV for the I.B.M. 7040 Digital Computer, was used to find solutions for the problem of second-order flow past a circular cylinder.

The input data required for this program is:

- OMGA(1) - Initial value of omega bar
- THTA(1) - Initial value of theta bar
- LM - Number of different values
 of theta bar
- LN - Number of different values
 of omega bar
- DTHTA - Increment of values of
 theta bar
- DOMGA - Increment of values of
 omega bar
- A(1),D(1) - Stagnation-point values of α
 and D
- DLTAS - Step-size for integration
 along body contour
- JM - Number of steps required
 to complete integration
- UINF - Magnitude of free-stream
 velocity

The output received from this program is:

- DEG - Degrees along cylinder
 corresponding to S
- S(I) - Curvilinear length along
 body surface

DRAG	- Cumulative record of viscous drag on cylinder
TAUW	- Wall shear stress, τ_w
DELTA	- Displacement thickness, δ^*
THETA	- Momentum Thickness, θ^*
ZETA	- ζ^*
D(I)	- Boundary layer thickness

```
C   COMPUTER PROGRAM FOR SECOND-ORDER FLOW PAST CYLINDER
    DIMENSION S(3000),A(3000),THTA(100),D(3000),OMGA(100)
    JM=2000
    LM=4
    LN=1
    THTA(1)=0.0001
    OMGA(1)=0.001
    DTHTA=0.02
    DOMGA=0.00
    UINF=1.0
    DLTAS=0.001
3   DO 200 M=1,LM
    GO TO (6,7,8,9,10,11,12,13,14), M
6   A(1)=3.1754
    D(1)=1.8778
    GO TO 15
7   A(1)=3.0743
    D(1)=1.7418
    GO TO 15
8   A(1)=2.9787
    D(1)=1.6066
    GO TO 15
9   A(1)=2.8868
    D(1)=1.4698
    GO TO 15
```

```
10 A(1)=2.9323
    D(1)=1.5385
    GO TO 15
11 A(1)=2.8868
    D(1)=1.4698
    GO TO 15
12 A(1)=2.8418
    D(1)=1.4000
    GO TO 15
13 A(1)=2.7973
    D(1)=1.3289
    GO TO 15
14 A(1)=2.7533
    D(1)=1.2560
    GO TO 15
15 CONTINUE
    4 DO 100 N=1, LN
        WRITE (6,51)
51 FORMAT (1H1/////55X22HVISCOSITY COEFFICIENTS//)
        WRITE(6,52) THTA(M)
52 FORMAT (1H 58X10HTheta BAR=F5.2)
        WRITE(6,53) OMGA(N)
53 FORMAT (1H 58X10HOMEGA BAR=F5.2)
        WRITE(6,54)
54 FORMAT(1H /// 8X7HDEGREES,7X3HDIB,11X4HDRAG,
```

```
17X11HTAU AT WALL,6X6HDELTA*,6X6HTHETA*,
26X5HZETA*,6X24HBOUNDARY LAYER THICKNESS)
5 DO 20 I=1,JM
  S(I)=0.0
  IF(I.EQ.1) GO TO 36
  S(I)=S(I-1)+DLTAS
  X1=(-A(I)**2/252.+A(I)/105.+4./35.)
  X2=((-2.*THTA(M))/(35.*D(I)**2))*(3.*A(I)**2-4.*A(I)+
148.)
  XA=X1+X2
  UE=2.*UINF*SIN(S(I))
  DUE=2.*UINF*COS(S(I))
  DRJ=0.0
  RJ=1.0
  X3=D(I)*(-A(I)/126.+1./105.)
  X4=((2.*THTA(M))/(35.*D(I)))*(6.*A(I)-4.)
  XB=X3+X4
  X5=(D(I)/20.)*(8.-A(I))
  X6=2.*D(I)*X1
  X7=(-2.)*D(I)*X2
  XR1=- (DUE/UE)*(X5+X6+X7)
  X8=D(I)*X1
  X9=(OMGA(N)/(35.*D(I)))*(3.*A(I)**2-4.*A(I)+48.)
  XR2=- (DRJ/RJ)*(X8+X9)+A(I)/(UE*D(I))
  XR=XR1+XR2
```

XC=THTA(M)*UE*A(I)**2/D(I)
XE=-THTA(M)*A(I)*UE
XS=12.-6.*A(I)+(THTA(M)-OMGA(N))*UE*A(I)**2*DRJ/RJ+
1(THTA(M)*A(I)**2+D(I)**2)*DUE
XF=1.0
XG=(-1./(D(I)*DUE))*(3.+OMGA(N)*A(I)*UE*DRJ/RJ)
XT=OMGA(N)*A(I)**2/(2.*D(I))*(DRJ/RJ-UE/DUE*(DRJ/RJ)*
1*2)+(D(I)/2.)*UE/DUE
XH=X1
XI=X3
XV=- (DUE/UE)*(X5+X6)-(DRJ/RJ)*(D(I)*X1+X9)+A(I)/(UE*D
1(I))
DSA=-6.+(THTA(M)-OMGA(N))*2.*A(I)*UE*DRJ/RJ+THTA(M)*
1DUE*2.*A(I)
DSD=2.*D(I)*DUE
DSR=- (THTA(M)*A(I)**2+D(I)**2)*UE+(THTA(M)-OMGA(N))*
1A(I)**2*(DRJ/RJ)*(DUE-UE*DRJ/RJ)
DEA=-THTA(M)*UE
DED=0.0
DER=-THTA(M)*A(I)*DUE
DHA=-A(I)/126.+1./105.
DHD=0.0
DHR=0.0
DFA=0.0
DFD=0.0

DFR=0.0
DIA=-D(I)/126.
DID=-A(I)/126.+1./105.
DIR=0.0
DCA=2.*THTA(M)*A(I)*UE/D(I)
DCD=-THTA(M)*A(I)**2*UE/D(I)**2
DCR=THTA(M)*A(I)**2*DUE/D(I)
DTA=(OMGA(N)*A(I)*DRJ/(D(I)*RJ))*(1.-(UE*DRJ)/(DUE*RJ
1))
DTD=((OMGA(N)*A(I)**2*DRJ)/(2.*D(I)**2*RJ))*((UE*DRJ
1/(DUE*RJ)-1.))+UE/(2.*DUE)
DTR=(OMGA(N)*A(I)**2/(2.*D(I)))*(DRJ/RJ)**2*(-(UE/DUE
1)**2+2.*UE*DRJ/(DUE*RJ)-2.))+D(I)*(UE/DUE)**2/2.+D(I)
2/2.
DGA=-OMGA(N)*UE*DRJ/(D(I)*DUE*RJ)
DGD=3./(D(I)**2*DUE)+(OMGA(N)*A(I)*UE*DRJ)/(D(I)**2*D
1UE*RJ)
DGR=-3.*UE/(D(I)*DUE**2)+(OMGA(N)*A(I)*DRJ)/(D(I)*RJ)
1*(-(UE/DUE)**2+(UE*DRJ)/(DUE*RJ)-1.)
DVA=D(I)*DUE/(20.*UE)+1./(UE*D(I))+(-A(I)/126.+1./105
1.)*(-2.*D(I)*DUE/UE-D(I)*DRJ/RJ)-OMGA(N)*DRJ*(6.*A(I)
2-4.)/(35.*D(I)*RJ)
DVD=(A(I)-8.)*DUE/(20.*UE)-A(I)/(UE*D(I)**2)-X1*(DRJ/
1RJ+2.*DUE/UE)+OMGA(N)/(35.*D(I)**2*RJ)*DRJ*(3.*A(I)**
22-4.*A(I)+48.)

DVR=((8.-A(I))*D(I)/20.)*((DUE/UE)**2+1.)-A(I)*DUE/(U
1E**2*D(I))+OMGA(N)/(35.*D(I))*(DRJ/RJ)**2*(3.*A(I)**2
2-4.*A(I)+48.)+D(I)*X1*((DRJ/RJ)**2+2.*(DUE/UE)**2+2.)

XW= (XG*XH-XI*XF)*DSD+(XF*XV-XH*XT)*DED+(XI*XT-XG*XV)
1*DCD+(XE*XF-XC*XG)*DVD+(XC*XI-XE*XH)*DTD+(XC*XT-XS*XF
2)*DID+(XS*XH-XC*XV)*DGD+(XE*XV-XS*XI)*DFD+(XS*XG-XE*X
3T)*DHD

XX= (XG*XH-XI*XF)*DSA+(XF*XV-XH*XT)*DEA+(XI*XT-XG*XV)
1*DCA+(XE*XF-XC*XG)*DVA+(XC*XI-XE*XH)*DTA+(XC*XT-XS*XF
2)*DIA+(XS*XH-XC*XV)*DGA+(XE*XV-XS*XI)*DFA+(XS*XG-XE*X
3T)*DHA

XY=((XG*XH-XI*XF)*DSR+(XF*XV-XH*XT)*DER+(XI*XT-XG*XV)
1*DCR+(XE*XF-XC*XG)*DVR+(XC*XI-XE*XH)*DTR+(XC*XT-XS*XF
2)*DIR+(XS*XH-XC*XV)*DGR+(XE*XV-XS*XI)*DFR+(XS*XG-XE*X
3T)*DHR)*(-1.0)

C NOW CALCULATE DA/DS AND DD/DS

DA=(XW*XR-XA*XY)/(XW*XB-XA*XX)

DD=(XX*XR-XB*XY)/(XX*XA-XB*XW)

36 CONTINUE

IF(I.GE.2) GO TO 37

DRAG=0.0

DA=0.0

DD=0.0

UE=2.*UINF*SIN(S(I))

X1=(-A(I)**2/252.+A(I)/105.+4./35.)

```
X5=(D(I)/20.)*(8.-A(I))
X8=D(I)*X1
X9=(OMGA(N)/(35.*D(I)))*(3.*A(I)**2-4.*A(I)+48.)
37 CONTINUE
A(I+1)=DA*DLTAS+A(I)
D(I+1)=DD*DLTAS+D(I)
DELTA=X5
THETA=X8
ZETA=X9/OMGA(N)
TAUW=UE*A(I)/D(I)
DEG=360.*S(I)/6.283
DRAGN=TAUW*SIN(S(I))
DLTDRG=((DRAG+DRAGN)/2.)*DLTAS
DRAG=DRAG+DLTDRG
WRITE(6,55) DEG,S(I),DRAG,TAUW,DELTA,THETA,ZETA,D(I)
55 FORMAT(1H 7XF6.2,7XF5.3,7XF8.4, 6XF8.4,7XF8.4,4XF8.4,
13XF8.4,12XF8.4)
IF(TAUW)50,21,21
21 CONTINUE
20 CONTINUE
50 CONTINUE
```

C HERE THRU 33 CALCULATES THE VELOCITY PROFILE

```
DIMENSION XN(200)
DO 17 I=1,JM,100
IF(I.EQ.1) GO TO 31
```

```
1486 DEGL=360.*S(I)/6.283
      IF(DEGL) 33,33,31
31 WRITE(6,32) S(I)
32 FORMAT(1H134X36HBOUNDARY LAYER VELOCITY PROFILE FOR ,
      120HDISTANCE ALONG BODY=F5.2///)
      WRITE(6,16)
16 FORMAT(54X,3HN/D,19X9HU OVER UE//)
      DLTAXN=0.10
      XN(1)=0.0
      DO 19 J=1,100
      ETA=XN(J)/D(I)
      RD=3.*A(I)
      RC=3.*A(I)-8.
      RB=6.-3.*A(I)
      UOUE=A(I)*ETA+RB*ETA**2+RC*ETA**3+RD*ETA**4
      XN(J+1)=XN(J)+DLTAXN
      WRITE(6,18) ETA,UOUE
18 FORMAT(50X,1H F8.4,16X1H F8.4)
      IF(XN(J)-D(I))19,19,17
19 CONTINUE
17 CONTINUE
33 CONTINUE
      OMGA(N+1)=OMGA(N)+DOMGA
100 CONTINUE
      THTA(M+1)=THTA(M)+DTHTA
```

200 CONTINUE

336 STOP

END

AN INTEGRAL METHOD FOR SOLVING THE BOUNDARY-LAYER EQUATIONS
FOR A SECOND-ORDER VISCOELASTIC LIQUID

By

Clarence Wesley Kitchens, Jr.

ABSTRACT

Assuming a polynomial of the fourth degree to describe the velocity function, the momentum integral equation for a second-order fluid is used to develop differential equations describing the boundary-layer for second-order flow past external surfaces. Using the momentum integral equation and appropriate boundary conditions, results are tabulated for both plane and axisymmetric stagnation flows. The effect of the second-order viscosity terms on the boundary-layer parameters for problems of flow past a circular cylinder and flow past a sphere is discussed. An interesting result is found in the case of flow past a sphere; for certain values of the second-order viscosity terms, there is a reduction in the viscous drag from that of Newtonian flow.